THERMODYNAMIC OPTIMIZATION OF DOWNHOLE HEAT EXCHANGERS FOR GEOTHERMAL POWER GENERATION

A Thesis Submitted to
the Graduate School of Engineering and Sciences of
Izmir Institute of Technology
in Partial Fulfillment of the Requirements for the Degree of

MASTER OF SCIENCE

in Mechanical Engineering

by
Slamet PARMANTO

August 2016
İZMİR

We approve the thesis of **Slamet PARMANTO**

Examining Committee Members:

_____
Prof. Dr. Gülden GÖKÇEN AKKURT
Department of Energy Systems Engineering, İzmir Institute of Technology

_____
Assist. Prof. Dr. Nurdan YILDIRIM ÖZCAN
Department of Energy Systems Engineering, Yasar University

_____
Prof. Dr. Serhan KÜÇÜKA
Department of Mechanical Engineering, Dokuz Eylül University

_____
Assoc. Prof. Dr. Erdal ÇETKİN
Department of Mechanical Engineering, İzmir Institute of Technology

_____
Assoc. Prof. Dr. Tahsin BAŞARAN
Department of Architecture, İzmir Institute of Technology

29 August 2016

_____ **Prof. Dr. Gülden GÖKÇEN AKKURT** Supervisor, Department of Energy Systems Engineering, İzmir Institute of Technology	_____ **Assist. Prof. Dr. Nurdan YILDIRIM ÖZCAN** Co-Supervisor, Department of Energy Systems Engineering, Yasar University
_____ **Prof. Dr. Figen KOREL** Head of Department of Mechanical Engineering, İzmir Institute of Technology	_____ **Prof. Dr. Bilge KARAÇALI** Dean of the Graduate School of Engineering and Sciences

ACKNOWLEDGEMENTS

ABSTRACT

THERMODYNAMIC OPTIMIZATION OF DOWNHOLE HEAT EXCHANGERS FOR GEOTHERMAL POWER GENERATION

Geothermal reservoirs have various thermodynamic and physical properties. The heat extraction and power generation from the geothermal reservoirs depend on the reservoir properties. Downhole heat exchangers (DHEs) are designed to move the heat extraction process into the geothermal well. The working fluid is injected to the DHE which suspends in the geothermal well, heated by geothermal fluid and then returned to the surface through the inner pipe. DHEs have been used for heating purposes widely but there is no application for electricity generation. Because of the natural convection on the geothermal fluid side, convective heat transfer coefficient is low and simultaneously the heat extraction rate is low comparing with extracting geothermal fluid by downhole pumps. Therefore if the temperature is high but flowrate is low in a geothermal well, DHEs are good alternatives to harness the energy from that well. Considering the number of wells with abovementioned conditions in the World, there is a potential for electricity generation coupling geothermal power plants with DHEs.

The main purpose of the Thesis is to develop a thermodynamic and economic evaluation model of DHEs for power generation and to examine the feasibility of the model. The thermodynamic model is developed by EES software and over 300 simulations have been conducted to identify the effects of the insulation, geothermal well conditions, geometry of DHE, mass flowrate and the type of working fluids to the performance of DHE system. The economic analyses are conducted to evaluate the thermodynamic results regarding the economic consideration such as Net Present Value (NPV), simple payback time and electricity production rate.

The results show that the insulation on the inner pipe is desirable to prevent heat loss along DHEs. The best design of the DHE is a design with deeper the depth, larger the diameter of the inner pipe, and higher mass flowrate for a specific geothermal heat source. The best design for the case study resulted as a work output of 3152 kW with annual net revenue and payback time of $1.75 million and 2.24 years, respectively. Besides, the economic evaluation gives positive value for NPV which means investment in DHE for geothermal power generation is acceptable.

ÖZET

JEOTERMAL ELEKTRİK ÜRETİMİ AMAÇLI KUYU İÇİ ISI DEĞİŞTİRGEÇLERİNİN TERMODİNAMİK OPTİMİZASYONU

Jeotermal rezervuarlar çeşitli termodinamik ve fiziksel özelliklere sahiptirler. Jeotermal akışkanın üretildiği rezervuarlardan alınabilen/aktarılabilen ısı miktarı ve bu ısıdan üretilen elektrik enerjisi miktarı rezervuar özelliklerine bağlıdır. Kuyu içi ısı değiştirgeçleri (KİID), jeotermal akışkandan ısı alımı/aktarımı işlemini kuyu içinde yapar. Kuyu içine indirilen farklı konfigürasyonlardaki borulardan oluşan KİIDne çalışma akışkanı gönderilir, bu akışkan jeotermal akışkan tarafından ısıtılır ve yüzeye geri dönerek ısıtma yada elektrik üretimi uygulamalarında kullanılabilir. Mevcut uygulamalar ısıtma uygulamaları olup herhangi bir elektrik üretimi uygulaması mevcut değildir. KİID uygulamalarında, kuyu içinde akış olmadığı için taşınım ile ısı transferi katsayısı düşüktür, bu nedenle çalışma akışkanına aktarılan ısı miktarı da kuyu içi pompa uygulamaları ile karşılaştırıldığında düşüktür. Dolayısı ile KİIDleri yüksek sıcaklıklı fakat düşük debili kuyulardan ısı alımı/aktarımı için iyi bir alternatiftir. Dünya'da mevcut bu özellikteki kuyular dikkate alındığında jeotermal santrallerin KİIDleri ile birlikte kullanımı elektrik üretimi için iyi bir potansiyeldir.

Tezin amacı, KİIDnin elektrik üretiminde kullanımı için termodinamik ve ekonomik bir model geliştirmektir. Termodinamik model EES yazılımında geliştirilmiş, geliştirilen termodinamik model üzerinde; boru yalıtımı, jeotermal kuyu özellikleri, KİID geometrisi, debi ve çeşitli çalışma akışkanlarının KİID performansına etkilerini belirlemek için 300'den fazla simülasyon gerçekleştirilmiştir. Termodinamik analiz sonuçları; net şimdiki değer, basit geri dönüş süresi ve elektrik üretim maliyeti gibi ekonomik parametreler için de analiz edilmiştir. Çalışmanın sonuçlarından biri KİID geri dönüş borusu üzerinde yalıtımın; ısı kaybı, dolayısı ile de çalışma akışkanı sıcaklığının düşümü açısında hayati olduğudur. Jeotermal akışkandan maximum ısı alımı için KİID tasarımında en uzun derinlik, en geniş iç boru ve en yüksek debi seçilmelidir. Örnek kuyu koşullarında simülasyonlar sonucu elde edilen en iyi durumda net iş üretimi 3152 kW, yıllık net geliri ve geri ödeme süresi sırasıyla 1.75 milyon dolar ve 2.24 yıldır. Ekonomik analiz sonucu, net bugünkü değer pozitif olduğundan, jeotermal elektrik üretimi için KİID yatırımı kabul edilebilir anlamına gelmektedir.

This Thesis

Dedicated to my beloved Father and Mother

TABLE OF CONTENTS

LIST OF FIGURES

LIST OF TABLES

LIST OF SYMBOLS

A	: Total heat transfer area (m^2)
a_{thick}	: Annulus thickness (m)
β	: Coefficient of thermal expansion
C^*	: Heat capacity rate ratio
C_{min}	: Minimum of C_c and C_h (kW/K)
C_{max}	: Maximum of C_c and C_h (kW/K)
c_p	: Specific heat (kJ/kg.K)
D_a	: Annulus diameter (m)
Dt	: Inner pipe diameter (m)
D_w	: Geothermal well diameter (m)
Dh	: Hydraulic diameter (m)
η_{gen}	: Generator efficiency
ε	: Heat exchanger effectiveness
f	: Friction factor
g	: Gravitational acceleration (m/s^2)
Gr	: Grashof number
t_{thick}	: Inner pipe thickness (m)
Ins_o	: Insulation thickness (m)
H	: DHE length (m)
k_t	: Inner pipe thermal conductivity (W/mK)
k_a	: Annulus thermal conductivity (W/mK)
k_{ins}	: Insulation thermal conductivity (W/mK)
h_f	: Heat transfer coefficient fluid ($W/m^2.K$)
L_{her}	: Hydrodynamic entry length (m)
L	: Length (m)
$\dot{m}$	: Mass flow rate (kg)
NTU	: Number of heat transfer unit based on C_{min}, UA/C_{min}
Nu	: Nusselt number
P	: Pressure (kPa)
Pr	: Prandtl number

q   : Heat flow rate (kW)

Ra   : Rayleigh Number

Re   : Reynolds number

T_i : Inlet temperature of the fluid stream (^{o}C, K)

T_o : Outlet temperature of the fluid stream (^{o}C, K)

T_w : Well temperature (^{o}C, K)

ΔT : Local temperature between two fluids (^{o}C, K)

ΔT_m : Log-mean temperature difference (^{o}C, K)

U   : Overall heat transfer coefficient (W/m^2.K)

v   : Kinematic viscosity (Pa.s)

W_t : Turbine work (kW)

Wnet   : Net Work (kW)

NPV   : Net Present Value

SPT   : Simple Pay Back Time

CHAPTER 1

INTRODUCTION

1.1. Overview of Geothermal Energy

Geothermal energy is the heat stored in the Earth. Resources of geothermal energy found a few kilometers beneath the Earth's surface. In the past, geothermal energy was used only for cooking and bathing until 1904 when Prince Piero Ginori Conti built and operated a tiny steam engine to generate electricity (DiPippo, 2012). Then, the development of geothermal technology in the World is rapidly increased.

The global geothermal power development continues to grow substantially, with the average growth up to 325.5 MW per year. Figure 1.1 shows geothermal installed capacity in the World. As of 2015, the geothermal electrical installed capacity in the World is over 13.3 GW and the potential global capacity could reach 18.3 GW by 2021 if all planned projects become operational (GEA, 2015).
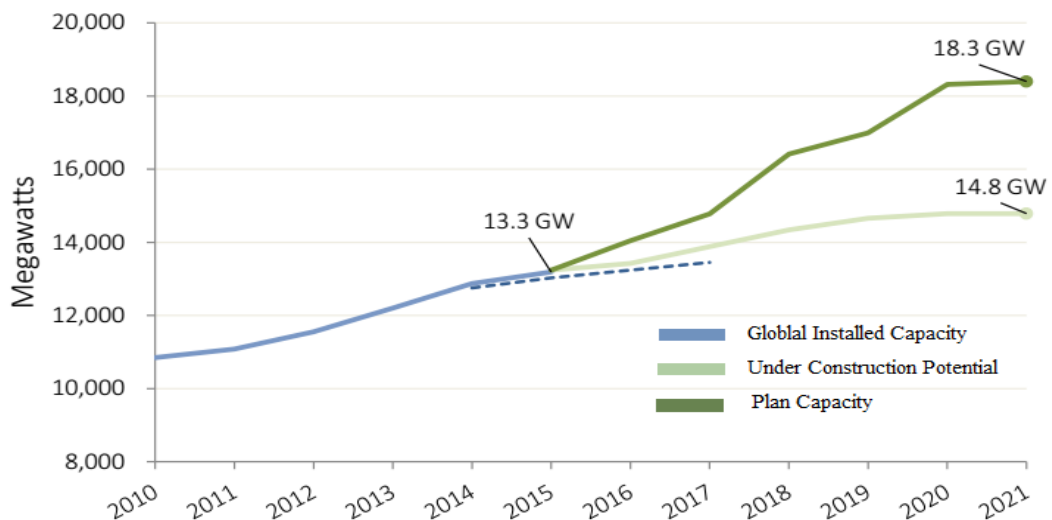
Figure 1.1. Global installed capacity.
(Source: GEA, 2015)

1.2. Energy Conversion System

Geothermal energy can be used for various direct use or power generation applications based on resource temperatures (Figure 1.2) such as fish farming, soil warming, and space heating as low-temperature applications, water distillation, dry ice production, and power generation as high-temperature applications.
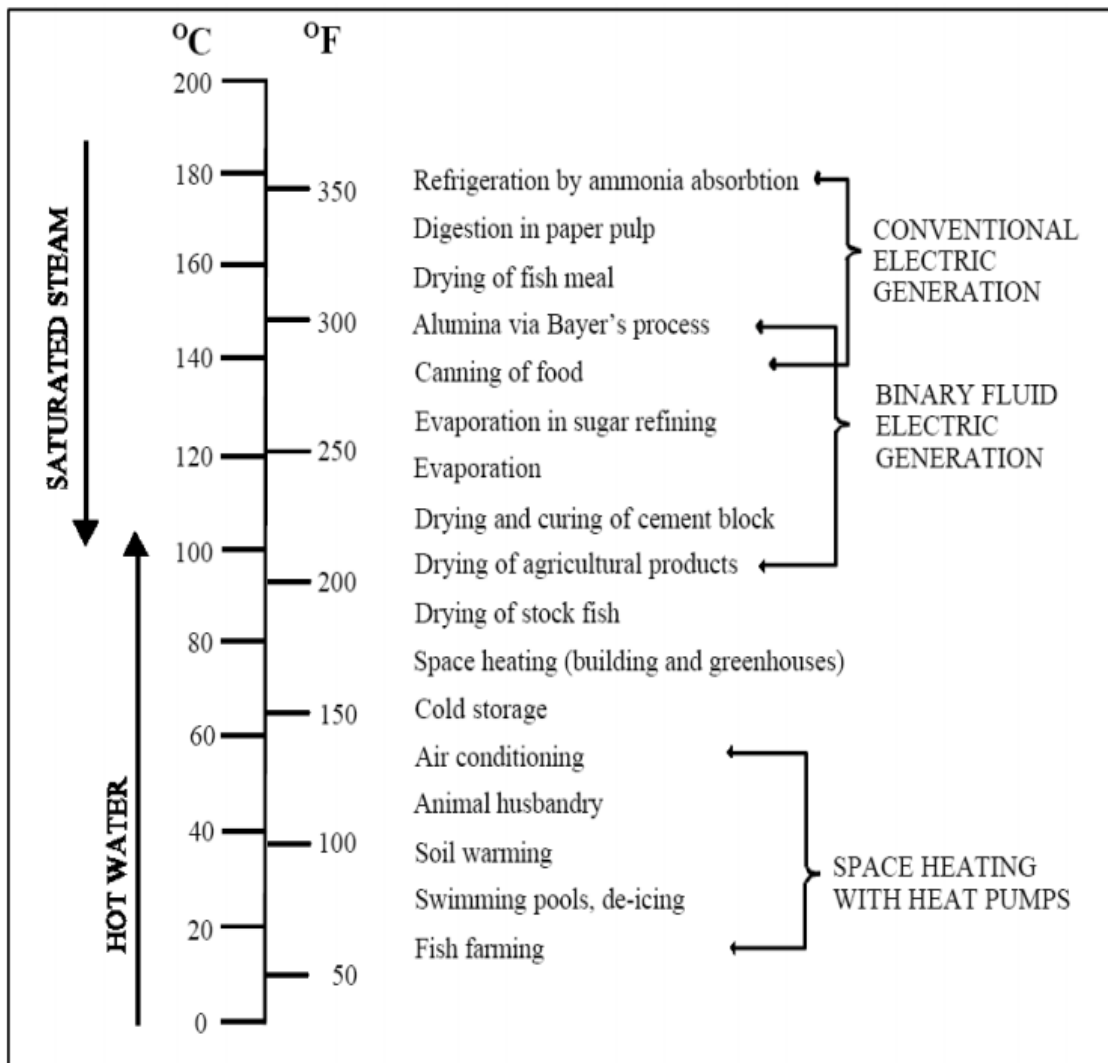
Figure 1.2. Lindal diagram.
(Source: Lund, 2010).

Electricity generation is one of the most common high-temperature application areas of geothermal energy. Conventional geothermal power plants use steam which is produced from the geothermal reservoirs at a temperature of >150°C. The steam rotates

a steam turbine which converts the thermal energy into mechanical energy. Then, the mechanical energy is converted into electricity by a generator. Basically, there are three types of geothermal power plants (GPPs); dry steam, flash steam, and binary geothermal power plants. The first type is dry steam GPPs which are the oldest and the simplest design. Dry steam GPPs use the steam that is produced in the reservoir (Figure 1.3). Low-pressure steam leaves the turbine first sent to the condenser, then can be re-injected back into the geothermal reservoir. This technology is used today at The Geysers (northern California) in the USA; Larderello and Monte Amiata in Italy; and Kamojang and Drajat in Indonesia.
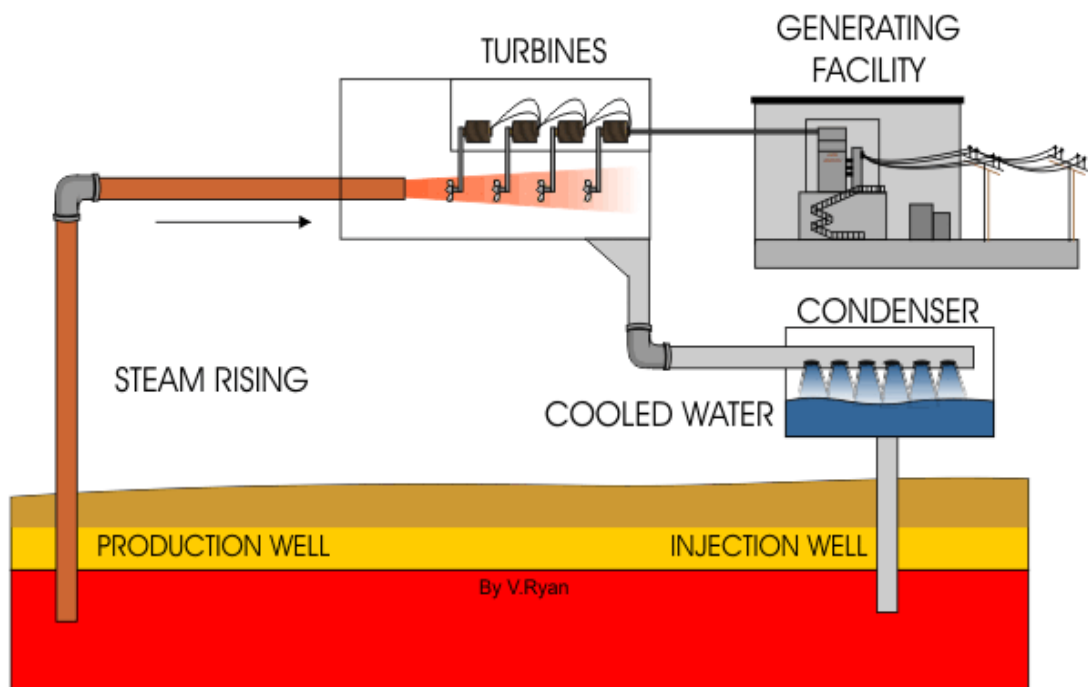
Figure 1.3. Dry steam power plant.
(Source: Ryan, 2009)

The second type is flash steam GPPs (Figure 1.4) which are the most common type of GPPs in the World. If geothermal wells produce a mixture of steam and liquid, a flash tank component (separator) is required to separate the steam and liquid phases. The separated steam is used to generate electricity while the liquid phase is injected into the reservoir or used for heating purposes. The example of flash steam GPPs are Wayang Windu and Ulumbu in Indonesia; Bacman Laguna in the Philippines; and Iwate and Hahijojima in Japan.
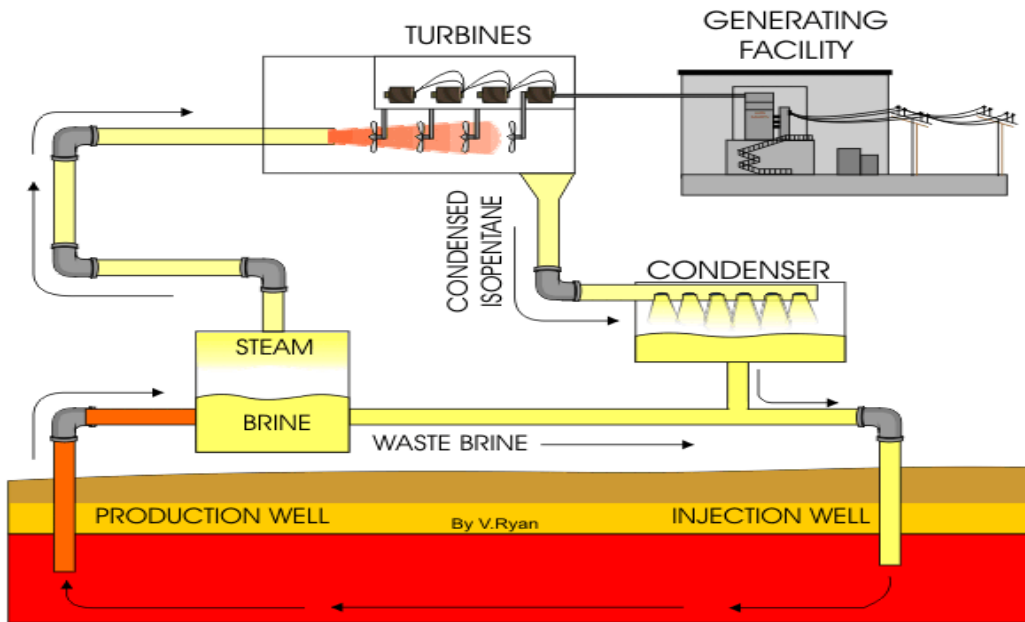
Figure 1.4. Flash steam power plant.
(Source: Ryan, 2009)
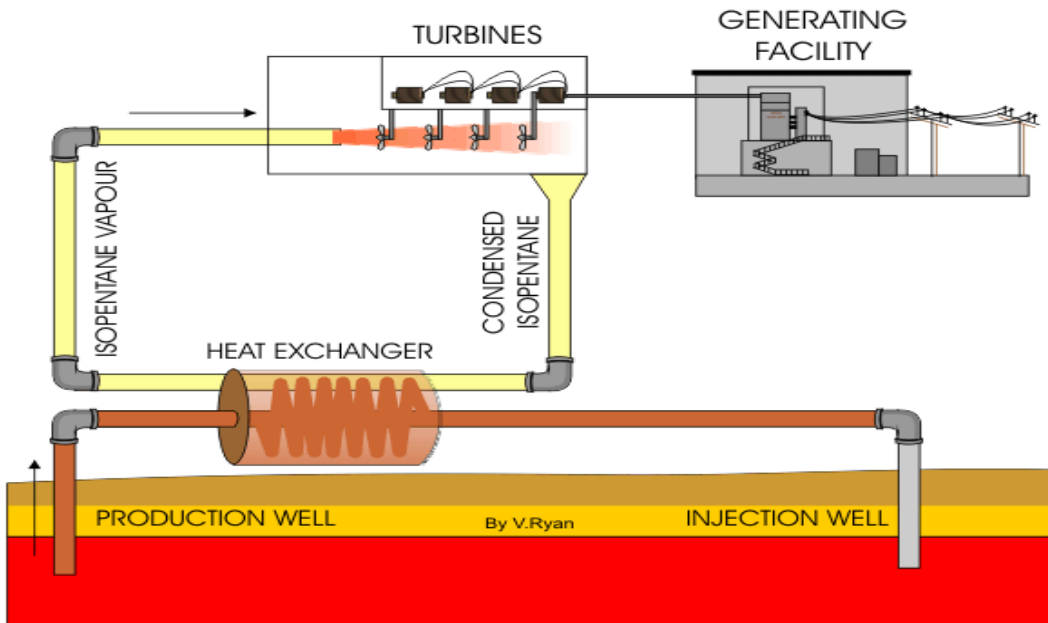
Figure 1.5. Binary cycle power plant.
(Source: Ryan, 2009)

The third type is binary GPPs (Figure 1.5) which are used if the reservoir temperatures are <150°C or chemistry of the geothermal fluid is harmful to the plant equipment. In a binary GPP, the geothermal fluid is fed into a heat exchanger where transfers its heat to a secondary working fluid at the second loop and then injected back

into the geothermal reservoir through an injection well. The secondary working fluid is evaporated at the heat exchanger exit, rotates the turbine to generate electricity, then in the condenser and then is sent to the heat exchanger back through a pump to complete the cycle (Boyle, 1996). The second loop is called the Organic Rankine Cycle (ORC) that basically resembles the steam cycle according to working principles. In ORC, working fluid is a necessary material since the heat transfers into it, which is a selection in working fluids becomes fundamental. Instead of water, in ORC is recommended to use a high molecular mass fluid with lower degree of boiling temperature in comparison with water such as refrigerant working fluids, hydrocarbons, and ammonia.

Figure 1.6 shows a T-S diagram of ORC. Stage 4-1 presents a heat exchanger or evaporator which changes the phase of working fluid from liquid to vapor by extracting heat from the heat source (hot brine liquid), turbine (1-2) which expand the steam and extracting power from it, condenser (2-3) which removes the heat from working fluid and condenses to liquid state, and stage 3-4 present a circulation pump that increases the liquid pressure before enter to heat exchanger.
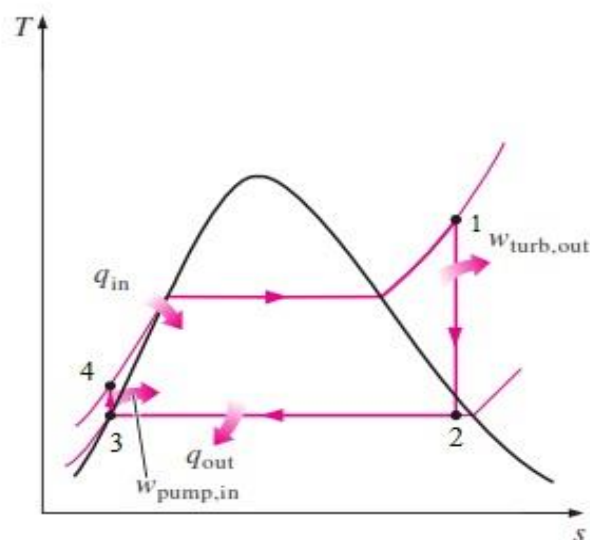
Figure 1.6. T-S Diagram of Organic Rankine Cycle.

The example of binary GPPs are Alasehir in Turkey; Ngatamariki in New Zealand; Tokamachi in Japan.

Besides the explained power plant types above, depending on the reservoir properties combined power plant such as flash and binary, double flash and triple-flash

GPPs can be installed. Flashed-steam (single and double-flash) GPPs are the most commonly used types of geothermal energy conversion system, composing 58% of the global GPP installed capacity (Figure 1.7).
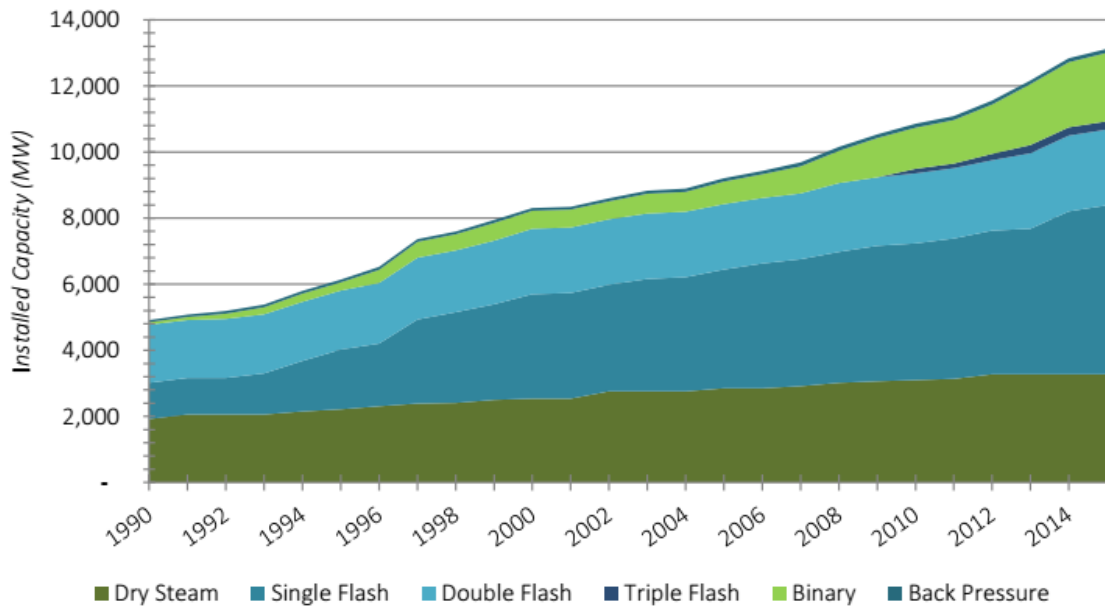
Figure 1.7. Type of GPPs and installed capacities.
(Source: GEA, 2015).

1.3. Challenges for Geothermal Energy Extraction

Conventional and binary GPPs require a sufficient flowrate along with the temperature for a feasible operation. If geothermal fields have high temperatures but low or no flowrate, they are called hot dry rock (HDR) systems. To be able to harness the energy stored from those fields, two deep wells are drilled, then water is injected down through one of the wells. The injection increases the fluid pressure in the naturally fractured rocks. Water passes by the hot rock, then returns back to the surface with an increase in temperature through the second well. After extracting its useful energy, the water is re-injected back to the injection well in order to extract more heat. This type of geothermal energy extraction is known as enhanced geothermal systems (EGS) (Figure 1.8).
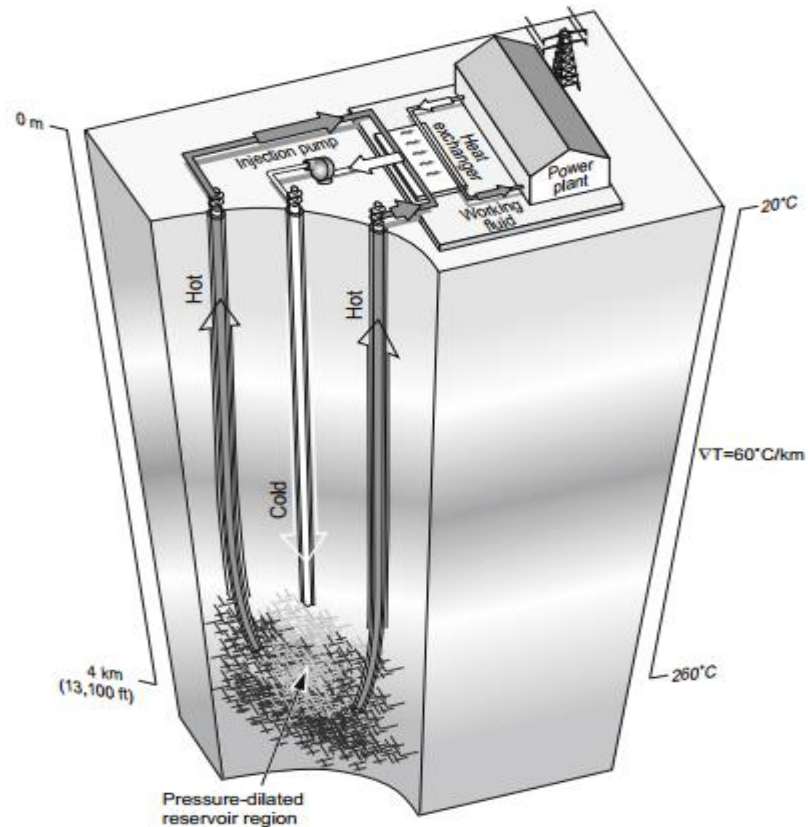
Figure 1.8. Conceptualization of EGS system.
(Source: Brown et al., 2012)

HDR system exists in many places around the World. According to Mertoğlu et. al (2015), technical and economical electricity production potential of HDR systems in Turkey (3-5 km of depth) is 250 GW_e that occurs in Menderes, Gediz, and Edremit graben areas. Manisa-Turkey in Gediz Graben is the area where the most of the discovered HDR systems exist. The depth, temperature and flowrate of the wells are 2400-3100 m, 180-263°C and 1-14 liter/s, respectively (Mertoğlu et. al. 2015). Globally, the total amount of heat contained from HDR is 800 times greater than the estimated energy content of all hydrothermal resources at economical depths (Duchane and Brown, 2002).

Besides EGSs, downhole heat exchangers (DHEs) can be applied to the HDR systems. Currently, this technology is applied to produce heat for direct use applications such as space heating, bathing, industrial process heating and snow melting but not to the power generation.

1.4. Downhole Heat Exchangers

A downhole heat exchanger (DHE) is designed to move the heat extraction process into the geothermal well. The working fluid is injected to the DHE which suspends in the geothermal well, then returned to the surface through the inner pipe. Downhole heat exchangers (DHEs) have been extensively used for direct use applications in the World. The installed capacity of DHEs were 70,328 MW_t (163,287 GWh/year) in 2015 which grew 1.62 times compared to installed capacity in 2010 (Lund and Boyd, 2016).

Besides direct use applications, DHEs can be a good alternative to harness the energy from geothermal resources when temperature is high but flowrate is low. DHEs have several advantages in extracting heat from the reservoir such as eliminating the problem of geothermal fluid discharge (corrosion and scaling problem) and re-injection well. Lastly, DHEs have a simpler design than binary GPPs which reduces the cost of the total investment. However, DHEs has one main disadvantage which is limited heat output compared to conventional downhole pump systems, since the flow rate is limited by the geometry of the DHE.

1.4.1. Types of DHEs

1.4.1.1. U-type DHEs

The U-type design is the most common type of DHE application (Figure 1.9). It consists of a pipe with U shape which suspends in the geothermal well. Then, the heat from the well is extracted to the surface by the working fluid that first injected into the U shape pipe. The promoter pipe is designed in order to obtain maximum heat output. Natural convection circulates the geothermal fluids through the perforations. Previous studies on effect of promoter to performance of DHE concluded that the heat efficiency of the DHE system can be improved by adding a promoter pipe (Lei et al., 2012; Lund, 1999). Figure 1.9 shows the typical DHE using U-type design with a promoter pipe.
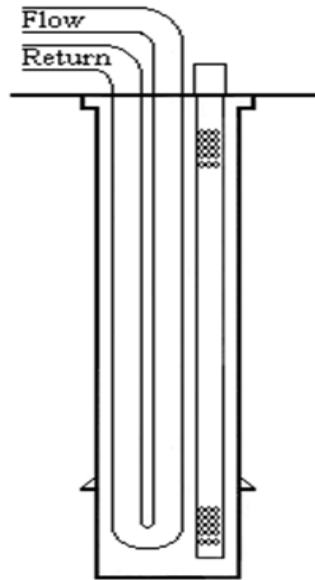
Figure 1.9. The U-type design of DHE with promoter pipe.
(Source: Alpay, 2002)

1.4.1.2. Multi-tube DHE

A multi-tube DHE consists of a shell with a bundle of tubes inside it. Working fluid runs through the tubes, and geothermal fluid flows over the tubes (through the shell) to transfer heat between the geothermal fluid into the working fluid. The set of tubes is called a tube bundle or multi-tube heat exchanger. In DHE application, a shell of multi-tube should be openly contacted with the geothermal fluid to let the each tubes extracting heat into working fluid. This type is capable of extracting more heat than U-type but causes a relatively high-pressure losses. Figure 1.10 shows a schematic of the multi-tube DHE that installed in Klamath Falls, Oregon-the USA.
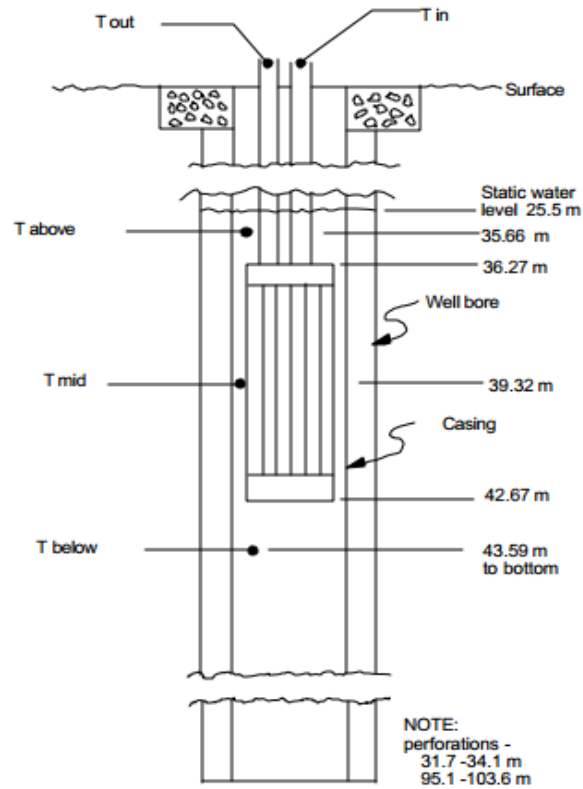
Figure 1.10. Schematic of multi-tube DHE in Klamath Falls.
(Source: Lund, 1999)

1.4.1.3. Coaxial DHE (CDHE)

Coaxial DHE consist of an inner steel pipe that is covered by an annulus pipe as a casing (Figure 1.11). Based on which pipe the working fluid is injected down, the flow called forward and reverse flow. In forward flow, the working fluid is injected down through the inner pipe and returns back to the surface from the annulus pipe after being heated by a hot rock or geothermal fluid. In reverse flow, the working fluid flows down through the annulus and goes up through the inner pipe. An experimental study on the thermodynamic performance of DHE types and configuration concluded that a reverse direction of coaxial DHE has greater performance compare with U-type and forward flow (Pan et al., 1982). Another advantage of coaxial DHEs over U type is the operation with higher flowrates.
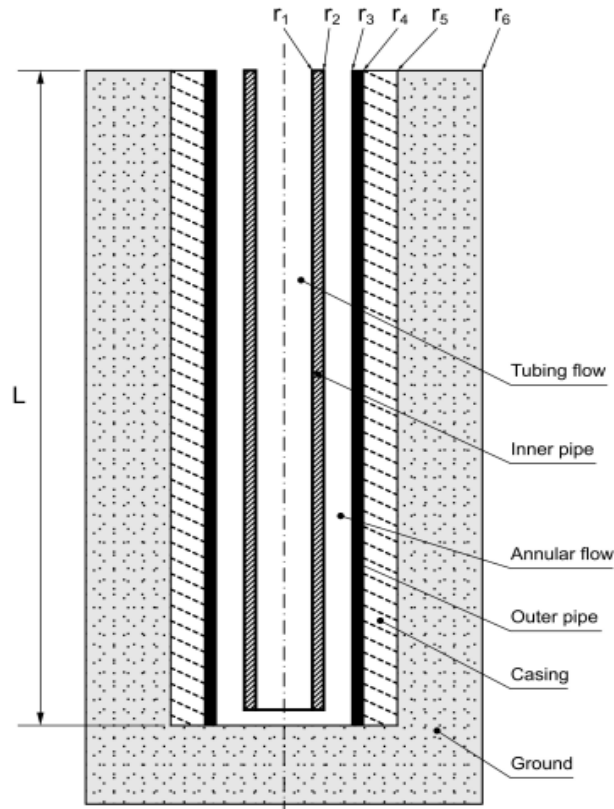
Figure 1.11. Conceptual drawing of Coaxial DHE.
(Source: Domínguez Masalias, 2010)

1.5. Thesis Objectives

The primary aim of the Thesis is to develop a DHE model for power generation to extract power from the high temperature but low mass flowrate geothermal resources. The objectives are to simulate the developed model thermodynamically based on DHE characteristics, well characteristics and working fluid characteristics, and show the economic feasibility of the model based on electricity sales price, net present value and simple payback time.

The Thesis consists of 5 chapters. Chapter 2 presents the literature survey while Chapter 3 gives the methodology of the Thesis. The results are presented and discussed in Chapter 4 and the study is concluded in Chapter 5.

CHAPTER 2

LITERATURE SURVEY

Literature survey will be giving as two main parts; the overview of the DHEs for direct use applications and thermodynamic optimization of the DHEs for power generation.

The aim of using DHEs is to extract heat from geothermal fluid. The influencing parameters on heat extraction rate are the geometry and configuration of DHE; temperature of geothermal fluid and depth of the well; and thermo-physical properties and flowrate of working fluids.

2.1. Direct Use

Most of the applications of the DHE are for direct use; such as space heating, snow melting and agricultural applications. The first study of the U-shaped bare steel pipe of DHE with a perforations pipe (promoter) was introduced by Culver and Reistad in 1978. The perforations pipe was installed after the casing to allow a circulation within the well, the study concluded that a well with perforation design had several times more heat output than the conventional solid-cased well (Culver and Reistad, 1978).

Other experimental studies on the effect of a promoter pipe also studied by Lei et al. (2012) and Lund (1999). The results of studies indicated that the thermal efficiency of DHEs can be improved by adding a promoter pipe.

Moreover, the studies showed that an increase in energy extraction rate can also be achieved by an increase resource temperature, well diameter and mass flow rate through the DHE (Lei et al., 2012; Lund, 1999).

The geometry of DHEs effects the diameter simultaneously flowrate and heat extraction rate of the DHE. Masalias (2010) considered the effect of the inner pipe diameter on the total entropy generation of the DHEs. The study resulted that for water as a working fluid, increasing the diameter of the inner pipe and thermal resistance minimizes DHE irreversibilities thus maximizes the exit temperature of the working fluid from the DHE. Similarly, Luo et al. (2013) examined the amount of heat exchange

between geothermal fluid and working fluid with the change in DHE diameter. The study concluded that heat exchange in DHE increases up to 7.1% by increasing the inner pipe diameter of DHE as expected because of increase in flowrate (Masalias, 2010; Luo et al., 2013).

The types of DHEs influence the performance of the DHE. Acuña (2010) investigated the effect of different types of DHEs between the U-type and coaxial DHEs. The study indicated that the coaxial DHEs present the advantage of better performance than a common U-type by minimizing the pressure drop up to 65% at all flow rates (Acuña, 2010). Additionally, Pan et al. (1982) also studied the effect of flow configuration on U-type, forward, and reverse flow of a coaxial DHE. The study concluded that reverse flow has greater energy extraction rate comparing with U-type, and forward flow.

Since heat transfer direction is from higher temperature side to lower temperature side in heat exchangers, care should be taken that in some parts of the DHE system, the geothermal fluid temperature could be lower than the working fluid. In this case working fluid loses heat to the geothermal fluid which decreases the heat extraction rate and insulation of the inner pipe become crucial. Morita et al. (1992), Guillaume (2011) and Zhe Wang (2010) investigated the performance of insulation for DHEs by performing measurements and numerical simulations. In the analyses, an insulation layer is placed on the inner pipe and the results indicate that the use of insulation has sufficiently high performance of DHE applications. When the insulation is applied to the inner pipe, the working fluid exit temperature from the DHE is much higher than without insulation case corresponds an increase in heat extraction rate.

2.2. Power Generation

Nalla et al. (2005) studied the potential of DHEs on electricity generation. The study considered the parametric sensitivity studies of operational and design parameters of DHEs such as; geometry, working fluid properties, circulation flowrates and well properties including basal heat flux, and rock formation type. The study showed that the working fluid residence time, heat transfer contact area and thermal properties of rock formation have significantly contributed to heat extraction rate.

Feng (2012) and Akhmadullin and Tyagi (2014) introduced a long horizontal DHE along for power generation with injected brine as a second heat source. The second

13

heat source from the brine is utilized to avoid the heat loss from the working fluid when the temperature of the formation near to the surface is quite low. The Feng's study has investigated the feasibility of a single well power production unit from low enthalpy geothermal resources. The DHE study provided three main controls; increasing the length of DHE that enhances the heat exchange area and prolong the residence time of working fluid, increasing the mass flow rate of working fluid, and increasing geo-fluid flow rate that increases the heat transfer rate of the system. Moreover, Akhmadullin and Tyagi's study also considered the selection of working fluid based on high thermal conductivity, high heat transfer, and safety. It gives n-Pantene as most suitable working fluid among other working fluids.

Pumping is required to circulate and to pressurize working fluid when it is injected to the DHE. But, operating circulation pump always consumes energy so that influences to the work output. In order to increase the work output, Morita et al. (2005) studied on minimizing pumping power for circulating working fluid to increase power generation. The diameter of the well and the inner pipe is a critical factor on pressure drop. The study concluded that the gravity head which arises in DHE is possible to substitute the pump function on circulating the working fluid.

In DHEs, working fluid selection is another important factor on heat extraction rate which is also a function of thermo-physical parameters of the working fluid. The ideal working fluid features have been widely studied in the literature. Kilicarslan and Müller (2005), Anh (2009), Masheiti (2011) and Karla et al. (2012) investigated the influence of working fluid on low to medium temperature Organic Rankine Cycle (ORC). Kilicarslan and Müller (2005) presented that water is a natural refrigerant with high heat content potential. But the refrigerants have several advantages over water such as reducing turbine size, increasing thermal efficiency, minimizing cooling water system, and possibility to operate at lower temperatures.

Anh (2009) studied several criteria for selection of working fluids; such as thermal efficiency, stability, compatibility with contacted materials in the cycle, safety, health, and environmental effects. In the study, hydrocarbons, alkanes, aromates, siloxanes, and cycloalkanes were selected for analysis. These working fluids have a compatibility, temperature range, environmental fluids and yield good thermal efficiency. Furthermore, the study showed that investigated alkanes, cyclopentane, toluene, and o-xclene are the most potential working fluids, depending on the working temperature range. Another

study on the effect of various refrigerants on the efficiency of geothermal power cycles were investigated by Masheiti et al. (2011) and Redko et al. (2016). Both studies concluded that the refrigerant R-245fa had a better performance.

Economical analysis is another important parameter in DHE design that should be considered when a new design is being built in order to obtain the feasibility of the design in terms of economic parameters. In the economical analysis, sizing component and selection of materials for DHE directly affect to the investment and operational cost. Karla et al. (2012) introduced thermo-economic modeling to investigate the high-potential of working fluids. The method provides a relation between thermodynamic performance with the levelized cost of electricity (LCOE) for various source temperature of organic Rankine cycle and working fluid.

Elíasson and Valdimarsson (2005) evaluated the economic feasibility of DHEs for electricity generation. The study indicated that the DHE is feasible when the sales price of electricity higher than 0.09 Euro/kWh.

The summary of literature studies that being use for the Thesis is given in Table 2.1.

Table 2.1. Summary of the literature survey.

Author	Year	Direct Use (DU) or Power Generation (PG)	Type of DHE	Type of Working Fluids	Explanation	Main Results
Acuña, J.	2010	DU	CDHE	water	Vertical DHE, theoretical	CDHE has better performance than U-type by minimizing ΔP up to 65%
Akhmad ullin, I., and Tyagi, M.	2014	PG	CDHE	R134a,R2 45ca,n-pentane,	Horizontal DHE, theoretical	The DHE with the counter flow scheme is the most efficient. N-pentane is the most suitable working fluid.
Anh, L. N.	2009			iso-pentane, n-pentane, tolune, p-xylene, n-butane, etc	Study on working fluids, theoretical	Alkanes, cyclopentane, toluene, and o-xcelene are the most potential working fluids

(cont. on next page)

Table 2.1. (cont.)

Culver and Reistad	1978		U-type	water	Vertical DHE, experimental	A perforated casing well gives more heat output than solid-cased well
Masalias	2011	DU	CDHE	water	Vertical DHE	Increase diameter and thermal resistance of inner pipe diameter minimize DHE irreversibility
Elíasso and Valdimarsson	2005				Economic analysis	The study indicates DHE is feasible for electricity when sales price > 0.09 Euro/kWh
Feng	2012	PG	CDHE	n-butane	Horizontal DHE, theoretical	The configuration of working fluid and brine flow in DHE is a key importance to DHE performance.
Guillaume	2011	DU	CDHE	water	Vertical DHE, experimental	Insulated inner pipe of CDHE resulted in sufficiently higher performance.
Kalra	2012	PG	U-type	Iso-butane	Study on working fluids, theoretical	Introduced thermo-economic modeling that resulted in a high geothermal source can be reduced CEP
Kilicarslan and Müller	2005	PG		R134a, R12, R22, and R152a, R718, etc	Study on working fluids, theoretical, ORC	Water is a natural refrigerant with high potential, but using working fluids instead water can increase η-th, reduce turbine size, etc
Lund	1999	DU	U-type	water	Vertical DHE, experimental	Multi-tube DHE is more economical to install in shallow wells with high-static water level
Luo and Rohn	2013	DU	U-type, CDHE	water	Configuration study, experimental	A bigger drillhole diameter has a better thermal performance than the smaller diameter that gives a performance about 6.7% and 2.16%, respectively.
Masheiti, Agnew, and Walker	2011	PG	CDHE	R-134a and R-245fa	Study on working fluid, theoretical	Refrigerant R245fa gives better performance by increasing thermal efficiency.
Morita et al.	1992	PG	CDHE	water	Vertical DHE, theoretical	The equivalent thermal conductivity of the pipe was estimated to be 0.06 W/m.K. In formation, q is dominated by pure conduction.
Morita et al.	2005	PG	CDHE	water	Vertical DHE, theoretical	Minimizing pumping power for circulating water is important. It is possible to use gravity effect on circulating working fluid.
Nalla et al.	2005	PG	CDHE	water	Vertical DHE, theoretical	Working fluid residence time, heat transfer contact area, geothermal well rock formation thermal properties have significantly contributed to heat extraction rate.
Pan et al.	1982	DU	U-type, CDHE	water	Vertical DHE, experimental	A reverse flow of CDHE has greater performance comparing with forward flow and U-type.

Table 2.1. (cont.)

Redko and Kulikova,	2016			R22, R143a, R218, R13b1, R318, etc	Study on working fluids, theoretical	For R600a/R141b mixtures indicates increasing of thermal efficiency up to 10-12% more
Wang et al.	2010	PG	CDHE	CO_2	Vertical DHE, theoretical	The heat transfer from the reservoir by convection dominates because of conduction through the rock to the wellbore is small, especially in the long term

As author's knowledge, although there are some theoretical studies on DHE application for power generation, there is no application yet. The objective of the Thesis to evaluate thermodynamic and economical analysis of DHE application for power generation in Turkey. A thermodynamic model of ORC with DHE system is developed based on a case study, validated and simulate for DHE well and working fluid characteristics, show the thermodynamic feasibility of the model. Besides the thermodynamic model, and economical analysis was conducted based on electricity sales price, net present value and simple payback time. The developed model allows the designer to simulate and optimize the power generation system with DHE conducting sensitivity analysis.

CHAPTER 3

METHODOLOGY

In this chapter; characteristics, assumptions and the methodology for thermodynamic and economic evaluation of the power generation with DHE (GPP-DHE) are described to examine the feasibility of the system.

3.1 Description of the System

The GPP-DHE consists of two sections; a DHE (I) and the power plant (II), as shown in Figure 3.1. The DHE (I) is a heat exchanger that extracts heat from a geothermal heat source and the power plant (II) converts the heat into useful work (electricity).
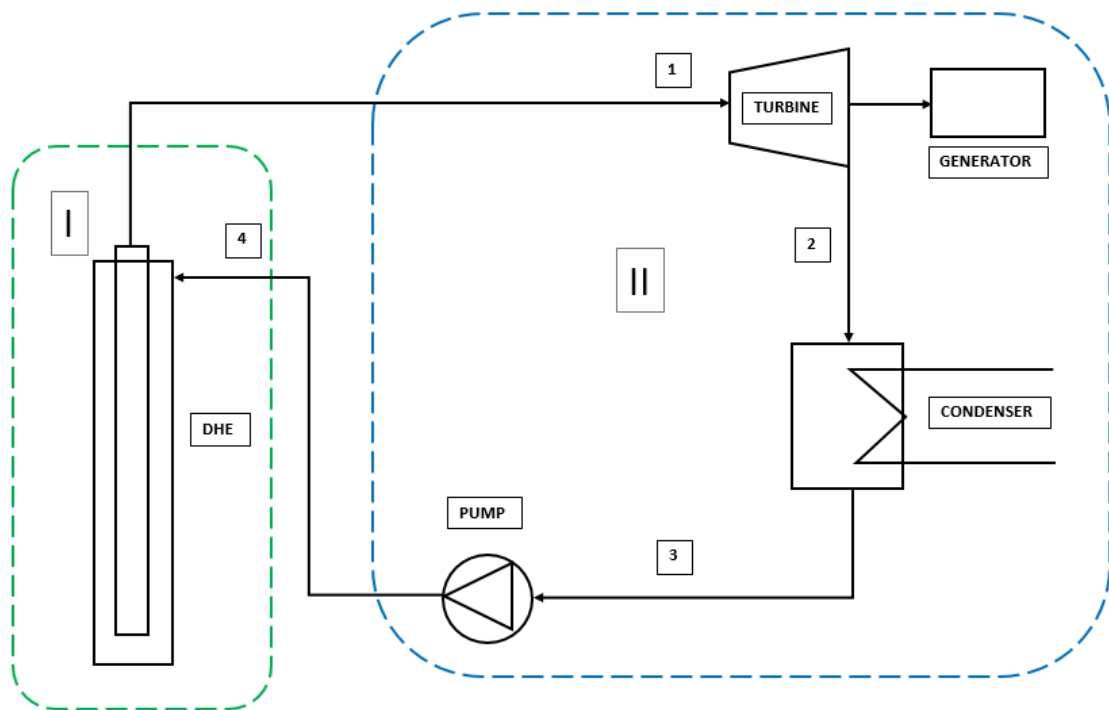
Figure 3.1. Schematic of the GPP-DHE.

The type of DHE is chosen as coaxial DHE due to the better performance than other types and configurations by minimizing the pressure drop (Acuña, 2010; Pan et al.,

1982) (Figure 3.2). The direction of the working fluid is the reverse direction where cold working fluid enters the annulus and exits through the inner pipe. To avoid temperature decrease at the DHE exit caused by heat loss from the working fluid the inner pipe is insulated.

The geothermal fluid in the well is not flowing but assumed as there is natural convection because of the changing temperature through the depth.
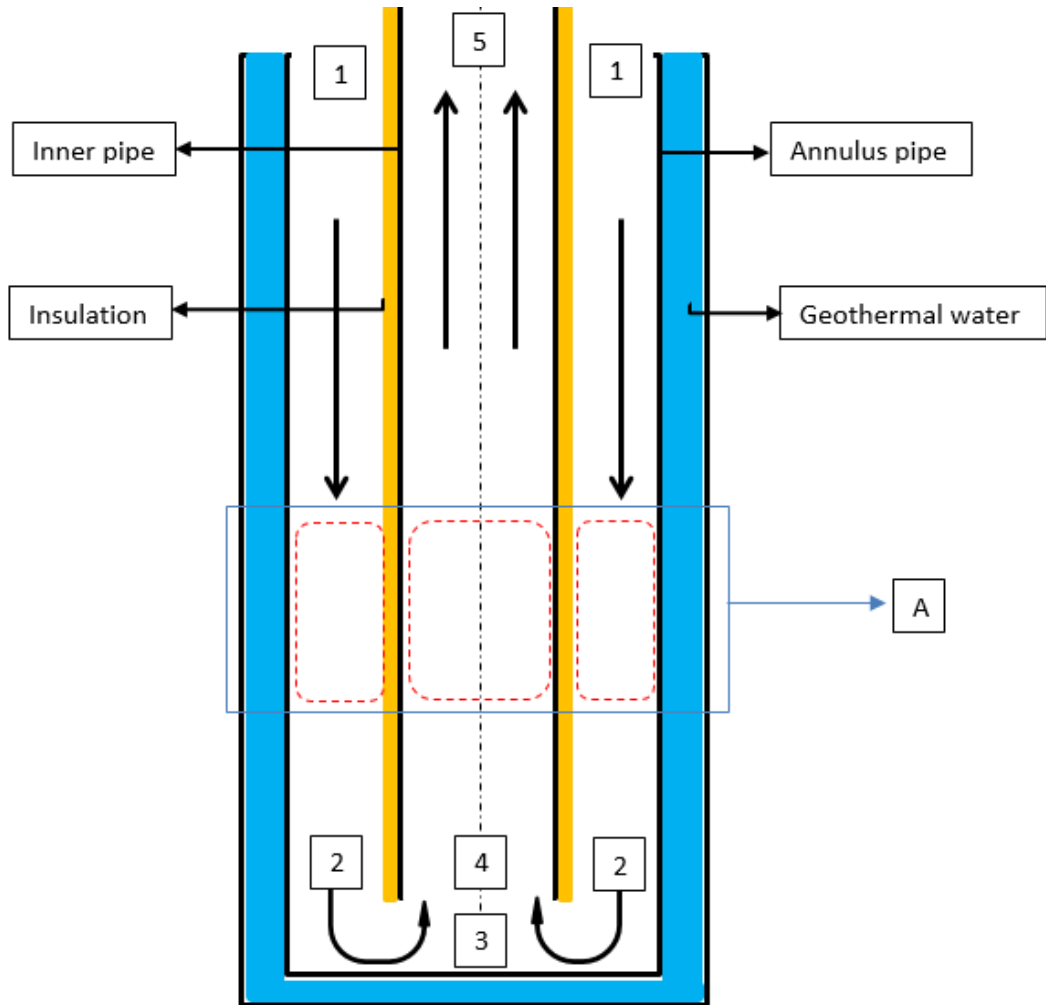
Figure 3.2. Schematic of the DHE.

Geometric parameters and thermal characteristics of DHE are summarized in Table 3.1. The insulation material is chosen as glass wool with a thin cladding (Figure 3.2). Geothermal well diameter is taken from an existing well. Depending on the well diameter, the annulus diameter is fixed. The length of DHE, inner tube diameter and pipe materials are taken as variable to evaluate their effect on heat extraction rate.

Table 3.1. DHE geometric parameter and properties.

Parameters	Unit	Value	Explanation (variable/fixed)
Inner pipe diameter (D_t)	(m)	0.1016-0.1524	Variable
Inner pipe thickness (t_{thick})	(m)	0.00655	Fixed
Insulation thickness (Ins_o)	(m)	0.002-0.012	Fixed
Annulus diameter (D_a)	(m)	0.2032	Fixed
Annulus thickness (a_{thick})	(m)	0.00818	Fixed
Geothermal well diameter (D_w)	(m)	0.254	Fixed
DHE length (H)	(m)	1000-3000	variable
Inner pipe thermal conductivity (k_t)	(W/mK)	4-231	variable
Annulus thermal conductivity (k_a)	(W/mK)	4-231	variable
Insulation (glass wool) thermal conductivity (k_{ins})	(W/mK)	0.043	Fixed

Figure 3.3 shows the thermal resistance network of an insulated cylindrical pipe where the insulation cause an increase in conduction resistance to the heat transfer while decreasing the convection resistance of the surface because of the increased outer surface area. The critical radius (r_{cr}) of insulation for a cylinder can be calculated by Equation 3.1. The thickness of insulation corresponding to the critical radius of insulation is known as critical insulation thickness. The rate of heat transfer from the cylinder increases with the addition of insulation if $r_2 < r_{cr}$, decreases for $r_2 > r_{cr}$ and reaches a maximum when $r_2 = r_{cr}$. The critical radius of insulation for a cylinder is calculated by Equation 3.1.

$$r_{cr} = \frac{k}{h} \tag{3.1}$$

Where k is thermal conductivity of insulation and h convective heat transfer coefficient (Cengel, 2007).
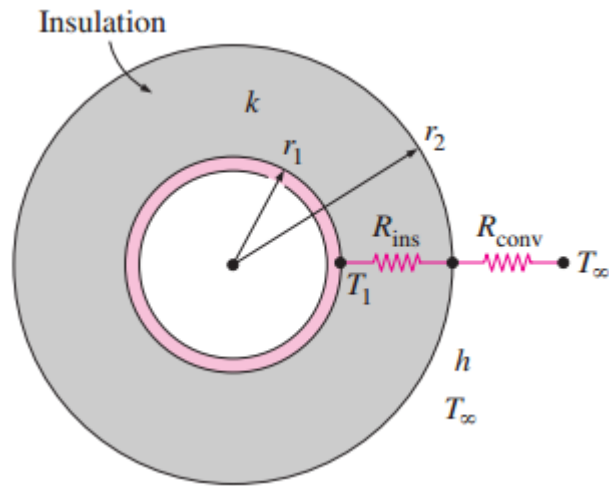
Figure 3.3. Thermal resistance network of an insulated cylindrical pipe.
(Source: Cengel, 2007)

3.2 Thermodynamic Model of the GPP-DHE System

The thermodynamic model of the GPP-DHE is based on the concept of log mean temperature difference. The overall thermal resistance is described into three components, inner pipe-annulus, annulus-geothermal fluid, and geothermal fluid-hot rock formation. However, it is assumed that the temperature profile of geothermal fluid is already determined during well tests so that thermal resistance between the geothermal fluid and hot rock formation is neglected. Energy balance is conducted for crosssection (A) in Figure 3.2. There exist two heat flows, one is from geothermal fluid to the annulus (q_1), the other one is from the inner pipe to the annulus or vice-versa (q2) (Figure 3.4).

The assumptions made for the model construction are;

- Energy balance is under steady state and steady-flow conditions.
- Fluid is assumed as a single phase.
- The geothermal fluid is in liquid phase.
- The thermal process in the geothermal fluid is governed by natural convection process and assumed as pure water
- The flowrate of the working fluid is constant.
- The temperature profile of the geothermal fluid is assumed as linear.
- q_2 is neglected because of the insulation on the inner pipe.
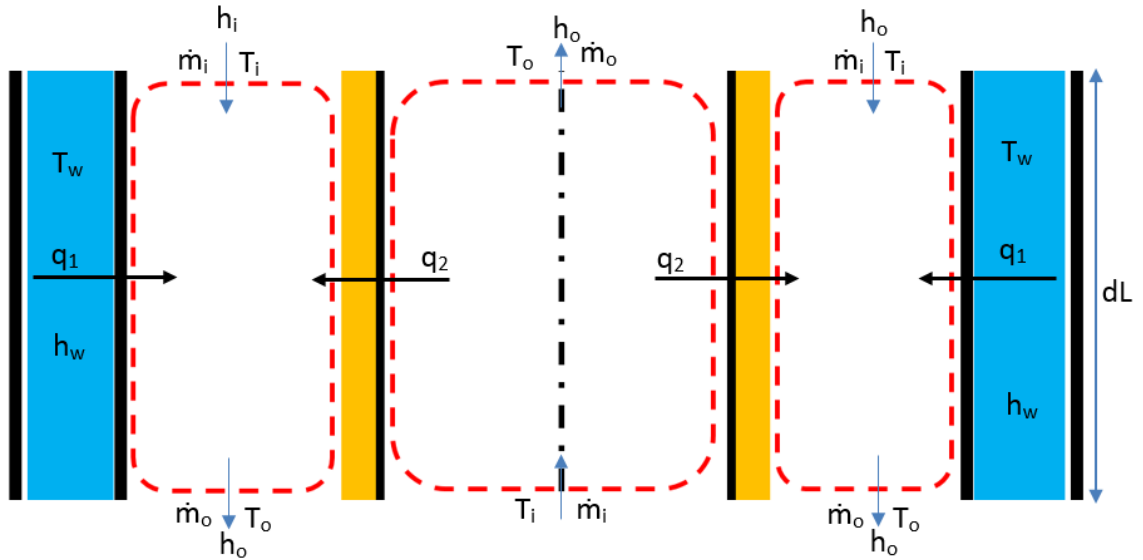
Figure 3.4. Heat flow diagram of two control volumes (q_1 and q_2) of the cross section A.

3.2.1 Energy Balance

Energy balance is applied to determine how the temperature of working fluid varies with position along the DHE (Kakac et al., 2012). From the first law of thermodynamics for an open system, under steady-state, steady-flow conditions, the energy balance for annulus control volume can be written as given in Equations 3.2.

$$E_{in} - E_{out} = \Delta E = E_1 - E_2 \qquad (3.2)$$

with no work interaction (W) added in the control volume and q_2 is neglected because of insulation, potential and kinetic energy changes are neglected, then Equation 3.2 simplifies to Equation 3.3.

$$0 = \dot{q}_1 + \dot{m}_i\, h_i - \dot{m}_o\, h_o \qquad (3.3)$$

and $\dot{m}_i = \dot{m}_o = \dot{m}$

then the energy balance for the annulus becomes as Equation 3.4.

$$\dot{q}_1 = \dot{m}(h_o - h_i) \qquad (3.4)$$

Where the rate of mass flow $\dot{m}$ into the control volume must be equal to the rate of mass flow out of the control volume, h_o and h_i represent the outlet and inlet enthalpies of the fluid stream which are function of temperature.

The temperature difference between hot and cold fluids $(\Delta T = T_h - T_c)$ varies with position in heat exchangers. Figure 3.5 shows the temperature distribution of counter and parallel flow heat exchangers with length. Therefore, log mean temperature difference (ΔT_m) is used for heat transfer analysis of heat exchangers. Heat transfer from hot stream to cold stream is calculated using Equation 3.5.

$$q = U.A.\Delta T_m \qquad (3.5)$$

Where A is the total heat transfer area (m²), U is overall heat transfer coefficient (W/m²K), ΔT_m (°C) is a function of T_{h1}, T_{h1}, T_{c1}, and T_{c2} (Figure 3.5).
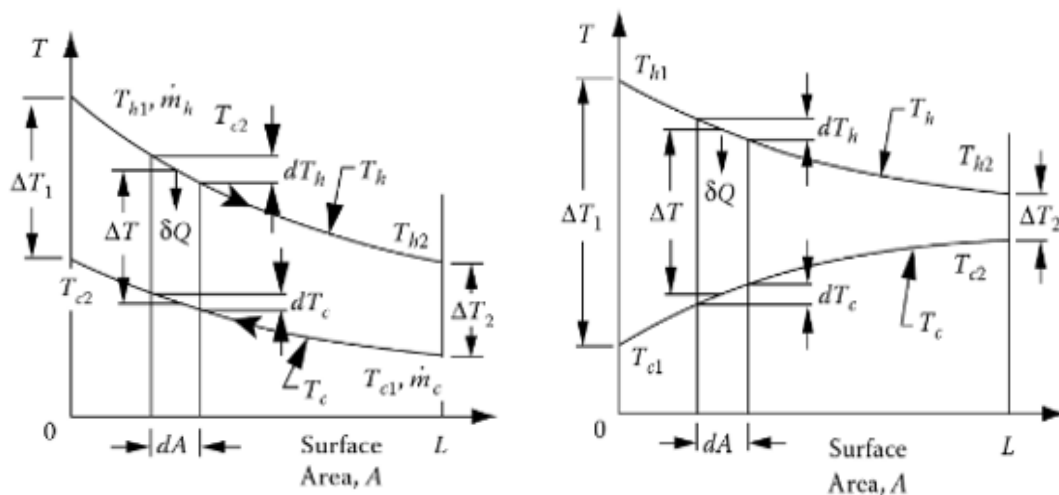
(a) Counter flow   (b) Parallel flow

Figure 3.5. Fluid temperature variation in counter flow and parallel flow.
(Source: Kakac et al., 2012)

The U of the annulus and inner pipe are calculated by Equations 3.6 and 3.7, respectively.

$$U = \cfrac{1}{\cfrac{1}{h_f} + \cfrac{D_a}{k} \ln \cfrac{D_{a,o}}{D_a} + \cfrac{D_a}{D_{a,o}.h_w}} \tag{3.6}$$

$$U = \cfrac{1}{\cfrac{1}{h_f} + \cfrac{D_t}{k} \ln \cfrac{D_{t,o}}{D_t} + \cfrac{D_t}{k_{ins}} \ln \cfrac{D_{t,ins}}{D_{t,o}} + \cfrac{D_t}{D_{t,ins}.h_{f\_o}}} \tag{3.7}$$

Where h_f is convective heat transfer coefficient of working fluid that will be defined in the next section.

3.2.1.1 Calculation of Convective Heat Transfer Coefficients

Working fluid flows in the annulus and inner pipe by forced convection while natural convection exist in the geothermal well. Laminar and turbulent forced convection correlations for single phase fluids represent a significant class of heat transfer solutions for heat exchanger analyses. Depending on the roughness of the pipe inlet and pipe surface, fully developed laminar flow will be obtained up to $Re \leq 2300$ if the pipe length L is longer than the hydrodynamic entry region L_{her}; however, if $L < L_{her,}$ developing laminar flow would exist over the entire pipe length. The Nusselt number for laminar flow, fully developed with a constant surface temperature is 3.66 for $Pr \geq 6$.

If $10^4 < Re < 5 \times 10^6$ and $0.5 < Pr < 2000$, the Nusselt number for turbulent fully developed flow becomes as Equation 3.8.

$$Nu = \frac{(f/8)(Re-1000)Pr}{1 + 12.7(f/8)^{1/2}(Pr^{2/3}-1)} \tag{3.8}$$

Where f is the friction coefficient that can be obtained from the Moody chart that provided by EES software database or by Equation 3.9.

$$f = (1.58 \ln Re - 3.28)^{-2} \tag{3.9}$$

Then, convective heat transfer coefficient h_f can be determined using Equation 3.10.

$$h_f = \frac{Nu.k}{D_h} \qquad (3.10)$$

Where k is thermal conductivity of working fluid and D_h is the hydraulic diameter of control volume.

Geothermal fluid flows "naturally" in the well as it is driven by buoyancy effect. The buoyancy arises due to the density differences which are the consequences of temperature or concentration gradients within the fluid.

Natural convection heat transfer in the well can be treated as a vertical plate (Kakaç et al., 1987) if Equation 3.11 applies.

$$\frac{D}{L} \geq \frac{35}{Gr_L^{1/4}} \qquad (3.11)$$

Where D is diameter and L is the length of the well. Nusselt number on a vertical plate can be calculated by Equation 3.12 and 3.13.

$$Nu_L = 0.508 Ra_L^{1/4} \left(\frac{Pr}{0.952 + Pr} \right)^{1/4} \text{ if } (Gr_L < 10^9) \text{ (for laminar flow)} \qquad (3.12)$$

$$Nu_L = 0.0295 (Ra_L)^{2/5} \frac{Pr^{1/15}}{(1 + 0.494 Pr^{2/3})^{2/5}} \text{ if } (Gr_L > 10^9) \text{ (for turbulent)} \qquad (3.13)$$

Ra_L is the local Rayleigh number which is defined by Equation 3.14.

$$Ra_L = Gr_L.Pr \qquad (3.14)$$

where,

$$Gr_L = \frac{g\beta(Tw - Tave)L^3}{v} \qquad (3.15)$$

Where Gr_L is Grashof number, g is gravity, β is coefficient of thermal expansion, and v is kinematic viscosity.

Heat transfer coefficient of the well h_w can be calculated by Equation 3.16.

$$h_w = \frac{Nu_L.k}{L} \tag{3.16}$$

3.2.1.2 The ε-NTU Method for DHE Analysis

The number of transfer units (NTU) is based on the concept of heat exchanger effectiveness, can be used for DHE analysis and calculated by Equation 3.17.

$$NTU = \frac{UA}{C_{min}} \tag{3.17}$$

Effectiveness (ε) of the DHE for counter and parallel flow can be calculated using NTU by Equation 3.18 and 3.19, respectively.

$$\varepsilon = \frac{1 - \exp[-(1-C^*)NTU]}{1 - C^* \exp[-(1-C^*)NTU]} \qquad \text{for counter flow} \tag{3.18}$$

$$\varepsilon = \frac{1 - \exp[-(1+C^*)NTU]}{1 + C^*} \qquad \text{for parallel flow} \tag{3.19}$$

Where C^* is capacity ratio that is calculated by Equation 3.20.

$$C^* = \frac{C_{min}}{C_{max}} \tag{3.20}$$

Where C_{min} and C_{max} are the smaller and larger of the two magnitudes of C_h and C_c, respectively, and $C^* \leq 1$.

The heat exchanger effectiveness can be calculated using Equation 3.21.

$$\varepsilon = \frac{q}{q_{max}} \tag{3.21}$$

Where q_{max} is maximum heat transfer rate that can be calculated using Equation 3.22.

$$q_{max} = C_{min}(T_w - T_i) \tag{3.22}$$

Knowing ε and qmax, the actual heat transfer rate q and exit temperature of control volume can be calculated using Equation 3.21 and 3.23, respectively.

$$T_o = T_i + \frac{q}{C_{min}} \tag{3.23}$$

3.2.2 Pressure Drop Calculations

The pressure drop of a vertical cylinder pipe (Figure 3.6) can be identified by three components; hydrostatic pressure drop (due to gravity), frictional pressure drop and kinetic pressure drop (Massoud, 2005). Kinetic pressure losses are minimal for most of the applications, therefore can be neglected. In the Thesis, kinetic pressure losses at the inlet and exit of DHE are neglected.

In downward flow, there exist frictional effects against the direction of flow, but the effective hydrostatic column helps the fluids to overcome such frictional losses. Hydrostatic pressure drop is a function of the density of the fluid and frictional pressure drop depends on the fluid properties and flowing conditions within the pipe.
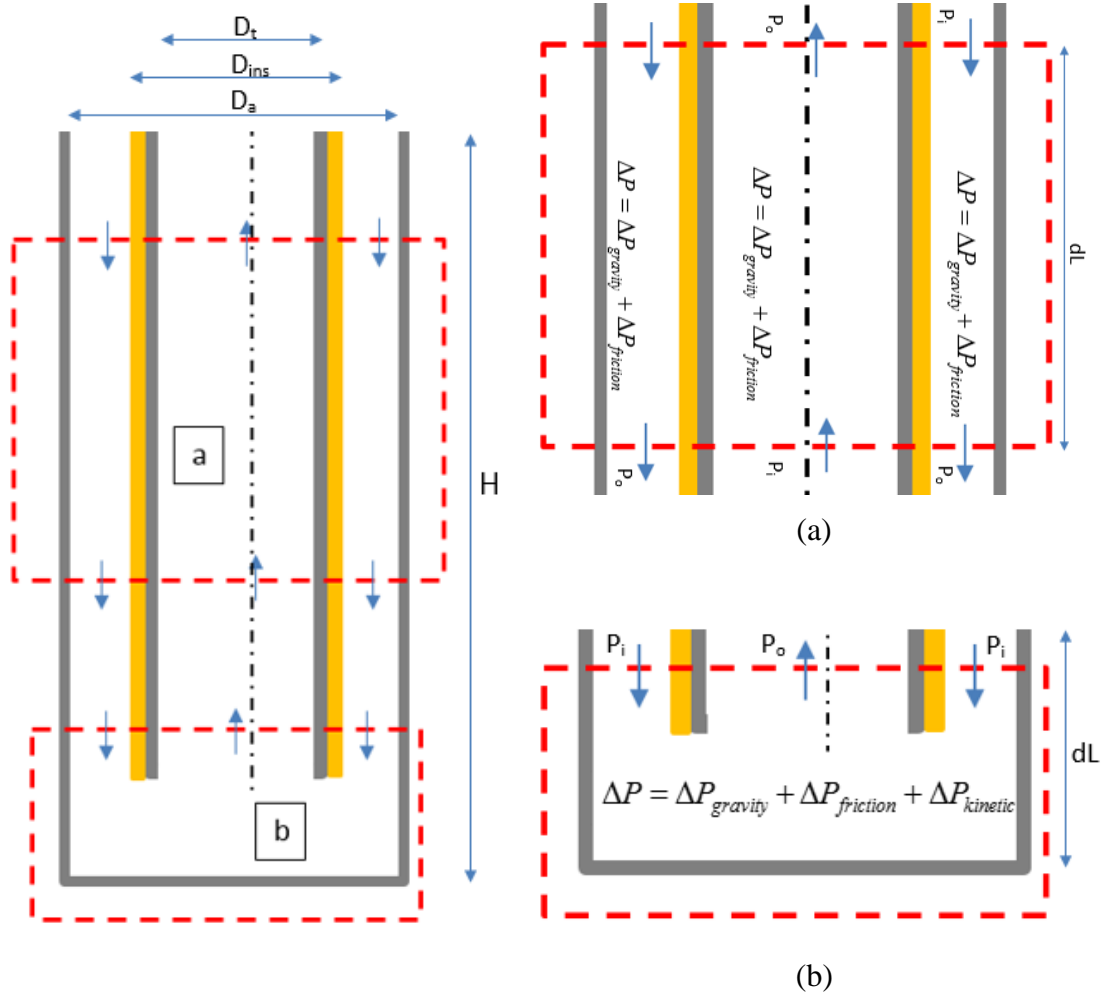
Figure 3.6. Detail of pressure drops in the channel of DHE; (a) pressure drop in the main channel (annulus and inner pipe region), (b) pressure drop in the bottom.

Pressure drop in the main channel for a vertical cylinder due to gravity and frictional losses can be determined by Equation 3.24.

$$\Delta P = \rho.g.L + \frac{(f.\rho.L.u^2)}{2Dh} \tag{3.24}$$

Pressure drop due to gravity occurs in the open systems, but it will cancel each other when it is a closed system when $\rho_{annulus} = \rho_{inner\ pipe}$. Since, the DHE is being heated by hot geothermal fluid which ρ will change by increasing temperature and pressure so that the pressure drop due to gravity still exists.

At the bottom of the DHE, a kinetic pressure drop occurs due to a change in the flow area. Hence, pressure drop at the bottom of the DHE is calculated by Equation 3.25

$$\Delta P = \rho.g.L + \frac{(f.\rho.L.u^2)}{2Dh} + \frac{\rho(\Delta V)^2}{2} \tag{3.25}$$

Pressure output (P_o) along the heat exchanger (L) can be determined by Equation 3.26.

$$P_o = P_i - \Delta P \tag{3.26}$$

3.2.3 Power Generation System

The working fluid temperature is increased in the DHE and sent to the power plant to generate electricity. The power plant corresponds to part II in Figure 3.2 and Figure 3.7. The power plant operates on the Rankine cycle and the main components of power generation system consist of a turbine and generator system, a condenser, and a feed pump.
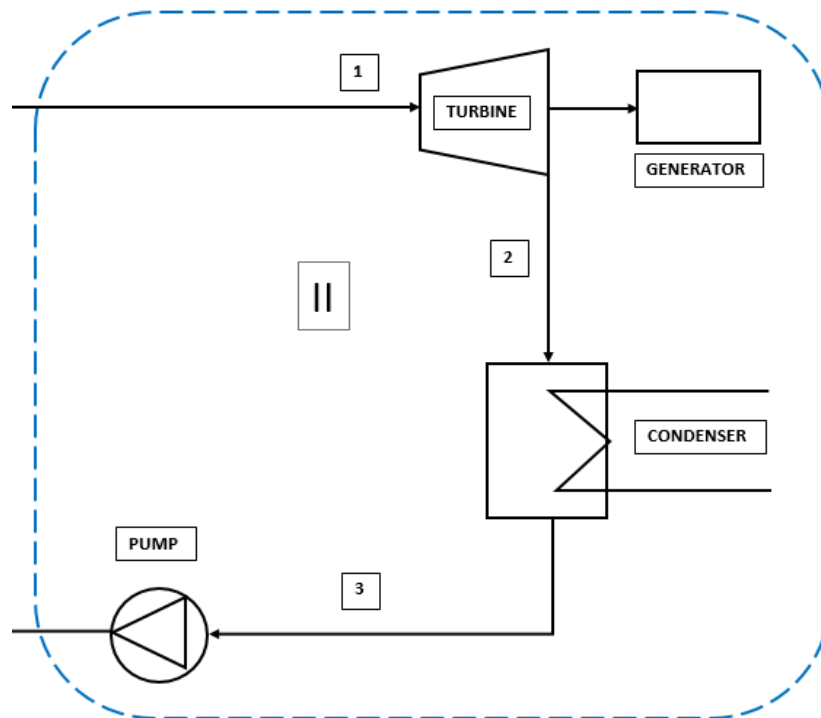
Figure 3.7. The power generation system.

3.2.3.1 Turbine analysis
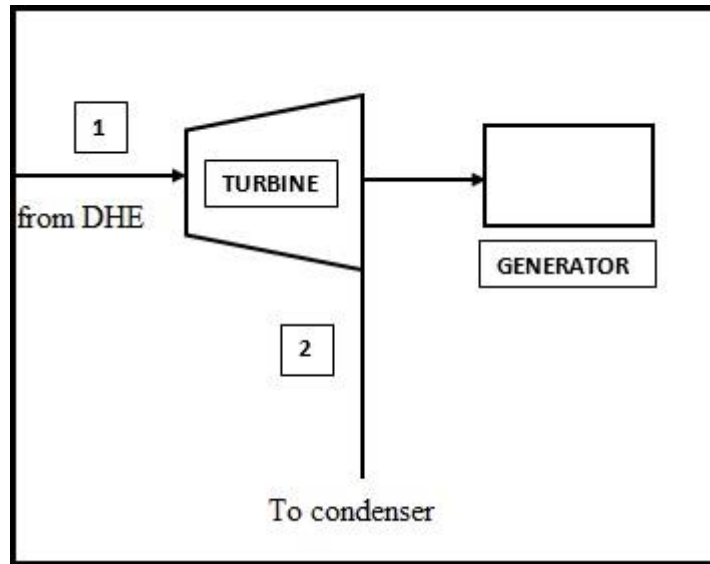
Figure 3.8. Turbine.

With the assumptions of negligible potential and kinetic energy terms together with steady, adiabatic operation, the energy balance equation simplifies to Equation 3.27 and 3.28.

$$W_t = \dot{m}_{wf}(h_1 - h_2)\eta_g \tag{3.27}$$

$$W_t = \dot{m}_{wf}\eta_t(h_1 - h_{2s})\eta_g \tag{3.28}$$

Where η_t is the isentropic turbine efficiency, η_g is the generator efficiency, $\dot{m}_{wf}$ mass flow rate of working fluids and h is enthalpy enter and exit of the turbine. A generator is a device that converts mechanical energy (from turbine) into electrical energy, which have high conversion efficiencies. In the Thesis, generator efficiency is assumed as 95%.

3.2.3.2 Condenser analysis
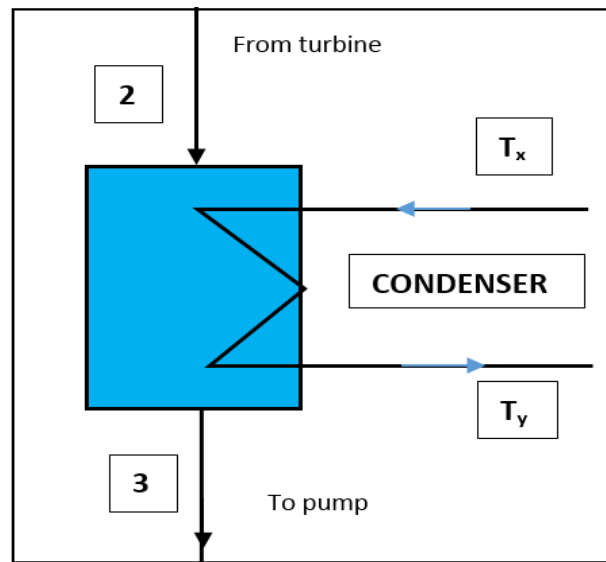
Figure 3.9. Condenser.

Condensers are used to convert steam at the turbine exit into liquid by cooling water. The performance of the condenser is quite important since the condenser temperature and pressure effect the turbine work and cycle efficiency.

The relationship between the flowrates of the working fluid and the cooling water is given by Equation 3.29.

$$\dot{m}_{cond}(h_y - h_x) = \dot{m}_{wf}(h_2 - h_3) \tag{3.29}$$

And the cooling water mass flow rate can be calculated by Equation 3.30.

$$\dot{m}_{cond} = \frac{\dot{m}_{wf}(h_2 - h_3)}{c(T_y - T_x)} \tag{3.30}$$

Where, T_x and T_y are the inlet and outlet temperature of cooling water.

3.2.3.3 Feed pump analysis

With the same assumptions as for the other components, the power needed the feed pump to circulate the working fluid into the DHE is calculated by Equation 3.31 and 3.32.

$$W_p = \dot{m}_{wf}(h_4 - h_3) \tag{3.31}$$

$$W_p = \dot{m}_{wf}(h_{4s} - h_3)/\eta_p \tag{3.32}$$

Where η_p is isentropic pump efficiency.

3.2.3.4 Net Work Output and Thermal Efficiency

The net work output is electricity power output after subtracted by electric power consumption for operating the feed pump.

$$W_{net} = W_t - W_p \tag{3.33}$$

Then the cycle performance can be assessed by the First Law using the thermal efficiency which is desired output over required input, the thermal efficiency can be calculated by Equation 3.34.

$$\eta_{th} = \frac{W_{net}}{Q_{in}} \tag{3.34}$$

A summary of the equations used for energy balance and pressure drop calculations based on Figure 3.2 is given in Table 3.2.

Table 3.2. Summary of equations for temperature and pressure distribution.

	Unit	Equation or (Equation Number)			Notes
		Point 1-2	**Point 3**	**Point 4-5**	
Temperature	D_h	$\dfrac{4A}{\pi D_a}$	D_a	D_t	Hydraulic diameter
	T_i	T_{inlet}	T_2	T_3	Temperature input
	Re	$\dfrac{4\dot{m}}{\pi \mu D_h}$	$\dfrac{4\dot{m}}{\pi \mu D_h}$	$\dfrac{4\dot{m}}{\pi \mu D_h}$	Reynolds number
	Nu	3.66 or (3.8)	3.66 or (3.8)	3.66 or (3.8)	Nusselt number for laminar or turbulent
	h_f	(3.10)	(3.10)	(3.10)	Convection heat transfer coeff at the point
	Gr_L	(3.15)	(3.15)		Grashof number
	Ra_L	(3.14)	(3.14)		Rayleigh number
	Nu_L	(3.12) or (3.13)	(3.12) or (3.13)		Nusselt number for laminar or turbulent flow
	h_w	(3.16)	(3.16)		Free convection heat transfer coeff at the well
	h_{f_o}			(3.10)	Convection heat transfer coefficient at annular region
	U	(3.6)	(3.6)	(3.7)	Overall heat transfer coefficient
	ε	(3.18) or (3.19)	(3.18) or (3.19)	(3.18) or (3.19)	Heat exchanger effectiveness
	q_{max}	(3.22)	(3.22)	(3.22)	Maximum heat transfer rate

(cont. on next page)

Table 3.2. (cont.)

	NTU	(3.17)	(3.17)	(3.17)	Number of heat transfer unit
	T_o	(3.23)	(3.23)	(3.23)	Temperature output
Pressure drop	ΔP_a	(3.24)			Pressure drop at main channel (point a)
	ΔP_b	(3.25)			Pressure drop at the bottom (point b)
	P_o	(3.26)			Pressure out
Rankine cycle	W_t	(3.27)			Turbine work
	W_p	(3.31)			Pump work
	η_{th}	(3.34)			Thermal efficiency

An example for DHE model calculation using EES software will be given in the Appendix B and C for 2500 m depth of DHE with 0.127 m diameter of the inner pipe, 64 kg/s R134a mass flow rate, and 3°C/50 m temperature gradient.

3.3 Economical Model

Geothermal power is one of the most desirable power generation technologies. A geothermal power plant has a zero cost of fuel and minimal maintenance cost. Besides that, it can be operated to generate electricity for over 30 years if the field is engineered and maintained sustainability (GEA, 2015). As like as the other project, the geothermal project has to be profitable. The most profitable project has to achieve a maximum revenue and emphasize all the expenses. In geothermal power, a maximum revenue means producing and selling much power, whereas to emphasize all the expenses may be achieved by reducing costs or increase the efficiency.

The DHE geothermal power plants are evaluated depending on Net Present Value (NPV), Simple Payback Time (SPT), and cost of electricity production rate.

3.3.1 Capital Investment Costs

The typical cost breakdown of geothermal power project depending on the site characteristics and condition of resources. The major cost components are shown in Figure 3.10.
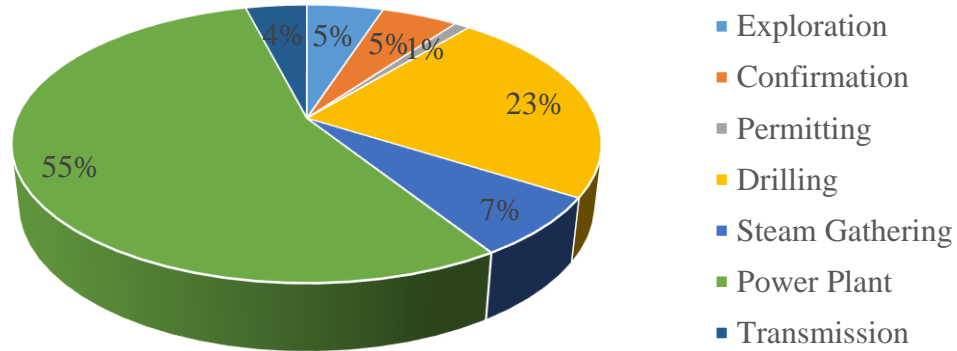
Figure 3.10. Capital investment cost components.
(Source: Hance, 2005)

The first step in a geothermal power project is the exploration. This step includes the field analysis and prospecting the geothermal resources. The results of the exploration are vital before begun the drilling process. The cost of exploration follows the nature condition and size of exploration activities.

Besides the cost for construction of power plant, the drilling process is one of the most costly processes in the geothermal power project. Geothermal resources are more uncertain, a long time process and have a high failure in the drilling process.

According to Hance (2005), drilling cost has range 600-1200 $/kW. In geothermal power, project permitting consists of legislative requirements such as environmental and construction issues (Konyalı, 2010). In Turkey, the unit range of the tender cost of permitting was 565-2030 $/kW in 2008 (Şener and Uluca, 2009).

The heat exchangers cost of DHE is calculated by multiplying the geometry of pipe with the current price of carbon steel pipe in the Turkey market (0.84 $/kg). The heat exchangers cost is different for every case, depending on the diameter and length of the DHE (Hatboru, 2016).

The steam gathering system is a network of pipes connecting the power plant with all production wells (DHE), included the circulation pump, reinjection pump, and

separator if it is necessary (Karadas, 2016). The cost of these facilities varies widely depending on the distance from the production and injection wells to the power plant, the flowing pressure, and chemistry of the produced fluids (Hance, 2005). The cost of the steam gathering system corresponds to over 5% of the total capital cost.

Power plant design and construction cost consist of the size and kinds of technologies. Field conditions (accessibility, topography, and local weather conditions) and resource characteristics also affect the cost. For the DHE power generation, the cost of power plant design includes the cost of the downhole heat exchangers. The transmission lines are quite expensive depending on how far the electricity is distributed.

The capital investment cost of geothermal power plants ranges from $1000-4000 $/kW, depending on the resource characteristics, technology, and temperature employed. The capital investment cost components and ranges of GPPs are summarized in Table 3.3.

Table 3.3. Capital investment cost components and unit cost range.
(Source: Hance, 2005)

Capital Investment Component	Cost Range ($/kW)	Average ($/kW)	
		Binary	DHE
Exploration	14-263	150	150
Confirmation	150	150	150
Drilling	600-1200	1000	1000
Permitting	565-2030	1000	1000
Design & Construction	1100-2700	1000	1000
Downhole Heat Exchanger	47-70	-	53
Steam Gathering System	30-400	150	50
Transmission		104	104
Total		3554	3507
Sub-Total (if the geothermal well already exists)		1254	1207

3.3.2 Operation and Maintenance Cost

The operation and maintenance costs include labor, administrative and cost of spares, the plant inefficiency, reservoir management costs, and cost of capital associated with increased working capital. Other cost components involve spending for consumable goods and any support service.

Maintenance costs are related to the maintenance of the system (pipe networks, turbine, generator, vehicles, buildings, and all services due to the maintenance process). The operation and maintenance cost components and ranges of GPPs are summarized in Table 3.4.

Table 3.4. O&M cost average value (5% inflation is adjusted).
(Source: Hance, 2005)

O&M Components	Average Cost (Cent/kWh)
Operating Cost	1.1
PP Maintenance	1.4
Steam field maintenance	1.3
Total	**3.8**

3.3.3 Economic Evaluation Methods

In addition to thermodynamic analysis, a financial evaluation is applied to the Thesis, in order to make a more comprehensive feasibility study. There exist various economic evaluation methods for the financial viability analysis of investments, which are based on some input values: revenues, interest rate, sales price, and capital investment costs. In the Thesis, NPV, electricity production cost rate, and SPT methods are used to evaluate whether the DHE power generation is competitive or not comparing with the other energy resources.

3.3.3.1 Net Present Value

NPV is the difference between the present value of the future cash flows and the amount of investment. It is an assessment of the expected addition to the investment wealth and used to decide whether an investment is profitable or better than other investments (Konyali, 2010). The NPV are expressed as Equations 3.35.

$$PV = \sum_{n=k+1}^{t} \frac{B_n}{(1+i)^n} - \sum_{n=0}^{k} (1+i)^n \qquad (3.35)$$

The project is accepted when NPV is a positive or greater than zero. Otherwise, the project is rejected.

3.3.3.2 Simple Payback Time (SPT)

The SPT refers to a period of time required to recover the initial investment, or to reach the break-even point. The method used to calculate simple economic payback time can be expressed as Equation 3.36.

$$SPT = \frac{Capital\ Investment\ Cost\ (\$)}{Annual\ Revenue\ \left(\frac{\$}{year}\right) - Annual\ O\&M\ Cost\ (\frac{\$}{year})} \tag{3.36}$$

The negative aspect of this method is that it does not consider the time value of money or neglected the discount of money during the period.

3.4 Methodology

3.4.1 DHE Program

The code is written in Engineering Equation Solver (EES) that has a high accuracy thermodynamic and transport property database that is provided for hundreds of substances in a manner that allows it to be used with the equation solving capability (Figure 3.11).

The numerical model is developed based on two main general flow diagram; the first is a numerical model of the DHE systems that results in temperature and pressure distribution along the depth of the downhole heat transfer, then the results would be used for second flow diagram, which is Rankine cycle calculation. The solution algorithm for development code of the model is given in the Figure 3.12.
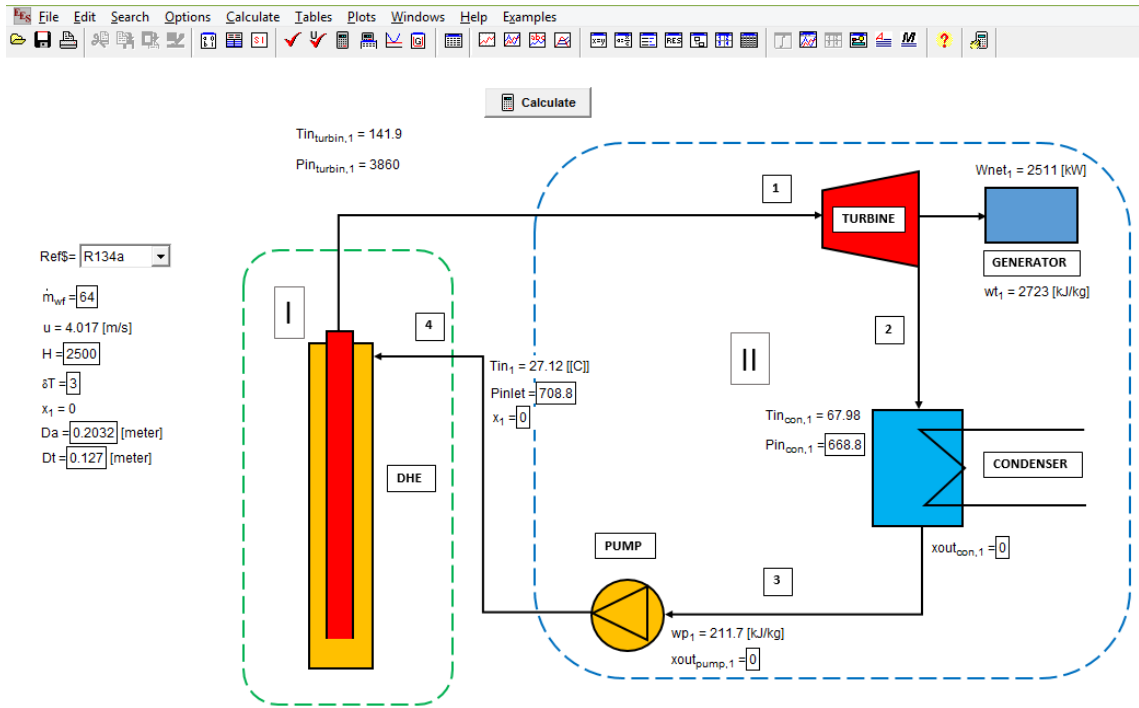
Figure 3.11. Diagram window view of the GPP-DHE developed by using EES Software.

```
                        ┌─────────────┐
                        │    Start    │
                        └──────┬──────┘
                               │
                               ▼
        ╱────────────────────────────────────────────╲
       │   • Well temperature profile (ΔT)            │
       │   • Geometry and properties DHE (H,          │
       │     L, Dt, Da, Insulation, k)                │
       │   • Mass flow rate of working fluid (ṁ)      │
       │   • Tinlet                                   │
       │   • Pinlet                                   │
        ╲────────────────────────────────────────────╱
                               │
                               ▼
              ┌────────────────────────────────┐
              │   Calculate number of grids    │
              │        N = (H/L)*2             │
              └────────────────────────────────┘
                               │
                               ▼
       ┌────────────────────────────────────────────┐
       │  Calculate physical properties of working  │
       │                  fluid                     │
       │   ρi, ui, ki, μi, Pri, fi, Rei             │
       └────────────────────────────────────────────┘
                               │
                               ▼
                          ◇ Rei < 2300 ◇
          NO  ◄──────────────           ──────────────►  YES
```

Decision: $Re_i < 2300$

NO branch:
$$Nu = \frac{(f/8)(Re-1000)\,Pr}{1+12.7(f/8)^{1/2}(Pr^{2/3}-1)}$$

YES branch:
$$Nu = 3.66$$

```
              ┌────────────────────────────────┐
              │  Calculate convection heat     │
              │   transfer of working fluid    │
              │              hf                │
              └────────────────────────────────┘
                               │
                               ▼
```

Calculate the film
temperature at geo-fluid
Tw

Calculate physical properties of working fluid
ρ_i, u_i, k_i, μ_i, Pr_i, f_i, Re_i

Calculate local Ra

$Ra_i < 10^9$

NO

YES

$$Nu_L = 0.0295(Ra_L)^{2/5} \frac{Pr^{1/15}}{(1 + 0.494\,Pr^{2/3})^{2/5}}$$

$$Nu_L = 0.508\,Ra_L^{1/4}\left(\frac{Pr}{0.952 + Pr}\right)^{1/4}$$

Calculate convection heat
transfer of geo fluid
h_w

41

Figure 3.12. Algorithm diagram for DHE system.

3.4.2 Overall Work Flow Diagram

Flow diagram of works is shown in Figure 3.13.

```
                    ┌─────────────────┐
                    │   Mass and      │
                    │ Energy Balance  │
                    └─────────────────┘
                             │
                             ▼
┌──────────────────┐  ┌─────────────┐  ┌──────────────────┐
│ Input            │  │             │  │ Output           │
│ Parameters:      │─▶│    DHE      │─▶│ Parameters:      │
│                  │  │   Systems   │  │                  │
│ Tw, H, Pinlet, ΔT│  │             │  │ Pout, Tout, ṁwf  │
└──────────────────┘  └─────────────┘  └──────────────────┘
                             │
                             ▼
┌──────────────────┐  ┌─────────────┐  ┌──────────────────┐
│ Input Parameters │  │             │  │ Output           │
│ (DHE) :          │─▶│   Rankine   │─▶│ Parameters:      │
│                  │  │    Cycle    │  │                  │
│ ṁwf, x, ηgen,Pcond│  │             │  │ Wt, Wp, Wnet, ηth│
└──────────────────┘  └─────────────┘  └──────────────────┘
                             │
                             ▼
┌──────────────────┐  ┌─────────────┐  ┌──────────────────┐
│ Input Parameters │  │  Economic   │  │ Economical       │
│ (Output of RC):  │─▶│  Analysis   │◀─│ Parameters:      │
│                  │  │             │  │                  │
│ Wnet             │  │             │  │ Sales price      │
└──────────────────┘  └─────────────┘  └──────────────────┘
                             │
                             ▼
                    ┌─────────────────┐
                    │    Capital      │
                    │  Investment     │
                    └─────────────────┘
                             │
         ┌───────────────────┼───────────────────┐
         ▼                   ▼                   ▼
┌─────────────┐      ┌─────────────┐      ┌─────────────┐
│   Annual    │      │  Cash Flow  │      │ Annual Cost │
│  Revenue    │      │             │      │             │
└─────────────┘      └─────────────┘      └─────────────┘
                             │
                             ▼
                     ┌─────────────┐
                     │ Annual Net  │
                     │  Revenue    │
                     └─────────────┘
                             │
         ┌───────────────────┼───────────────────┐
         ▼                   ▼                   ▼
┌─────────────┐      ┌─────────────────┐  ┌─────────────┐
│     NPV     │      │ Cost of         │  │     SPT     │
│             │      │ Electricity     │  │             │
│             │      │ Production Rates│  │             │
└─────────────┘      └─────────────────┘  └─────────────┘
```

Figure 3.13. Work flow diagram of the Thesis.

3.4.3 Parametric Sensitivity Study and Assumptions

Several sensitivity analyses are carried out to analyze the performance of the DHE power generation, such as; effect of insulation in the inner pipe, depth of DHE, the temperature gradient of the well, diameter of the inner pipe, mass flow rate and type of working fluids, and economic analysis. The results are being used to evaluate the feasibility of the DHE system for power generation.

General assumptions:
- ✓ Flow is assumed as a single phase.
- ✓ The thermal process in the geothermal fluid is governed by natural convection process and assumed as pure water.
- ✓ The temperature profile in the geo-fluids region is assumed as linear by the depth of the well.
- ✓ Steady-state conditions are valid.

Sensitivity study:
- Effect of insulation, pipe materials and flow direction.
  - ✓ Variable parameter: $thick_{ins}$: 0.2-1.2 cm k_{pipe} : 4-231 W/m.K
  - ✓ Fixed depth: 2500 m
  - ✓ Mass flow rate: 30 kg/s
  - ✓ Type of working fluids: R134a
  - ✓ Output: temperature and pressure distribution
- Depth and temperature gradient
  - ✓ The temperature profile in the geothermal water region is assumed as linear by the depth of the well.
  - ✓ Depth parameters: 1000-3000 with increment every 500 m.
  - ✓ ΔT parameters: 2-5°C/50 m with increment every 0.5°C.
  - ✓ Working fluid: R134a with mass flow rate : 30 kg/s.
  - ✓ Output: Wnet (kW)
- Effect of geometry
  - ✓ Variable parameter: Dt: 0.1016, 0.127, 0.1524 m
  - ✓ Fixed depth: 2500 m

✓ Mass flow rate: 15 kg/s

✓ Type of working fluids: R134a, R22, R125, R245fa, n-Pentane, n-Butane

Table 3.5. Assumptions for operating condenser and pump pressure.

Working Fluids	P_{inlet} condenser (kPa)	P_{outlet} pump (kPa)	References
R134a	668.8	708.8	Maclaine-Cross and Leonardi (1997)
R22	1091	1131	Maclaine-Cross and Leonardi (1997)
R125	1637	1677	Baik et al. (2011)
R245fa	249.6	289.6	Bahrami et al. (2013)
n-Pentane	116.3	156.3	Bahrami et al. (2013)
n-Butane	250	290	Tola and Finkenrath (2015)

✓ Output: U (W/m^{2}K), T and P distribution.

- Optimum mass flowrate and type of working fluid
    ✓ Variable parameter: ṁ: 10-70 with increment every 5 kg/s
    ✓ Dt: 0.1016, 0.127, 0.1524 m
    ✓ Working fluid: R134a, R22, R125, R245fa, n-Pentane, n-Butane
    ✓ Thermodynamic properties of working fluids are summarized in Appendix A
    ✓ ΔT: 3°C/50 m
    ✓ Output: Optimum ṁ (kg/s), Wnet (kW), η$_{th}$ (%)
- Power generation
    ✓ The steam gathering system is assumed short and well insulated (no heat loss during carrying heat into the turbine from DHE)
    ✓ The generator is set in 95% efficiency
    ✓ Isentropic efficiency of circulation pump is 85%
    ✓ Output: Wnet (kW)
- Economic analysis
    ✓ The economic model uses the highest net work output of each case.
    ✓ Assumed that the well already exists, which means exploration, drilling, and permitting cost are no included in the calculation.

- ✓ The capacity factor of electricity production is 95%.
- ✓ The interest rate at 10% is assumed constant for 20 years life of the plant.
- ✓ Variable parameter: sales price: 0.055-0.105 $/kWh
- ✓ Annual O&M cost is assumed constant.
- ✓ Inflation and amortization costs are not taken into account.
- ✓ Output: total investment costs, net revenue, SPT, cost of electricity production rate.

CHAPTER 4

RESULTS AND DISCUSSIONS

In this chapter, the thermodynamic and economical analyses of the model are given in detail. These analyses are made to investigate the feasibility of DHE for power generation. The model is validated by Guillaume's study.

4.1 Validation of the Model

A coaxial downhole heat exchanger (CDHE) with a depth of 184 m has been experimentally studied by Guillaume in 2011. The annular DHE has been installed in Lidingö, north of Stockholm-Sweden and is also simulated by COMSOL software.

To verify the model developed in the Thesis, Guillaume's study is used.

4.1.2 Characteristics of CDHE Installation in Lidingö

The CDHE consists of two modules of polyethylene pipe (Figure 4.1) that surrounded by the ground (hot rock). The first module is an annular pipe, which is designed very thin and direct contact with the ground to obtain a better heat exchange between the ground and the working fluid. The diameter of this pipe is 115 mm.

The internal pipe is about 5 m from the bottom of the hole, where the diameter is 40 mm. In order to reduce heat loss between two modules, an insulation with 8 mm thickness is applied in the half-length of the internal pipe. In the experiment, water at a constant flow rate is used as a working fluid with 2.1 l/s mass flow rate.

To measure temperatures, a Distributed Temperature Sensing (DTS) with fiber optic cables have been placed in the central pipe, on the external pipe, and between the external pipe. The measurements include;

- Temperatures of the fluid inside the inner pipe, the fluid inside the external pipe, and temperature on the borehole wall.

- Water flow rates on the water loop.

Internal pipe
Insulation
Curragated plastic
Water
External pipe
Ground
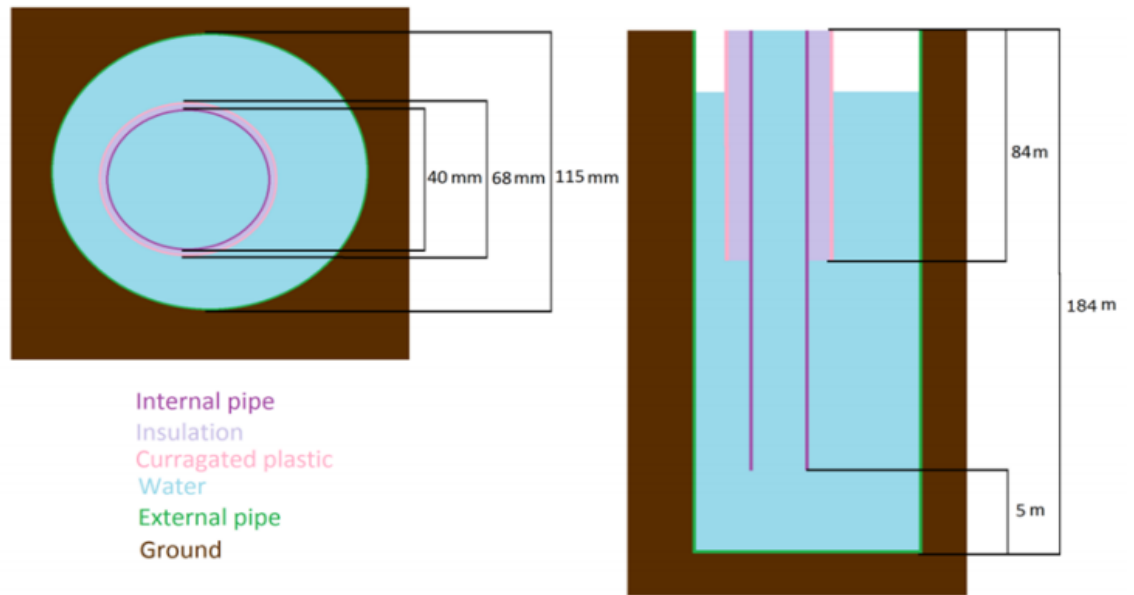
Figure 4.1 Dimension of the CDHE in Lidingö.
(Source: Guillaume, 2011)

The temperatures are recorded every 2 minutes and each 4 m. The borehole wall temperature profile (Figure 4.2) and characteristics of the wall are adopted to the EES model developed in the Thesis.
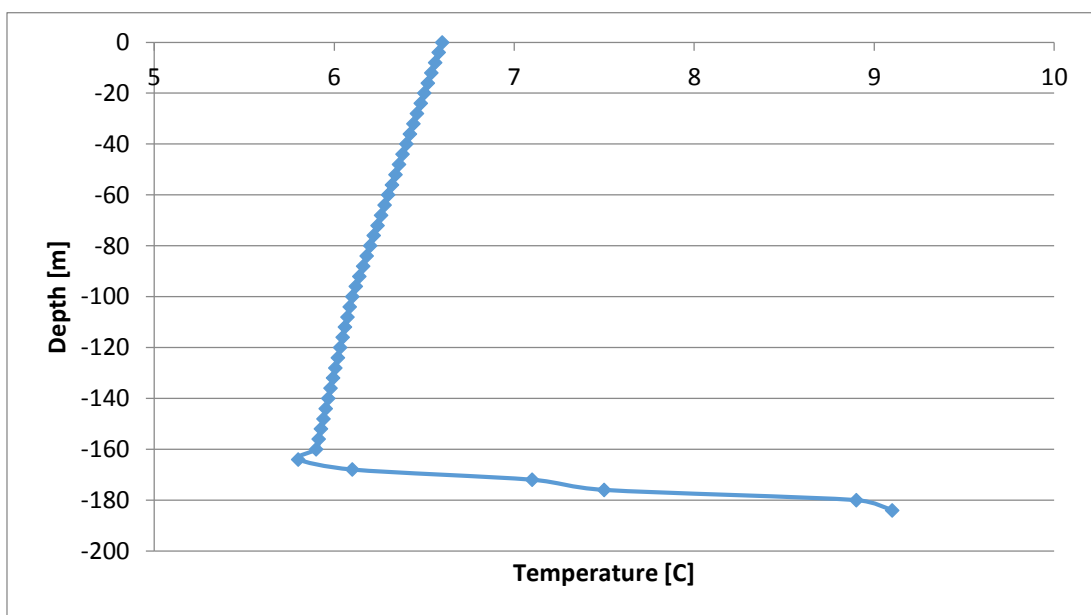
Figure 4.2. The borehole wall temperature profile.
(Source: Guillaume, 2011)

4.1.3 Comparing the Model with Measurement and Comsol Results

Figure 4.3 represents a comparison between the EES model which is developed in the Thesis and the measurement and Comsol given by Guillaume (2011). The measurements show that the working fluid goes down with an inlet temperature approximately 4.77°C and slightly increases after extracting heat from the ground. Then the fluid reaches the bottom of the borehole and goes up to the surface with a temperature of approximately 5°C and 6.35°C, respectively. There is an amount of water which is nearly undistributed by the flow of working fluid. So that, there is a temperature jump in between the bottom of the external pipe and internal pipe. The temperature of the fluid is very close to the temperature of the borehole wall.

The same conditions also applied for the simulation, an inlet temperature is set with 4.77°C. Then, the temperature increases due to the extracting heat from the ground. Comparing with Comsol, the EES model result gives better outlet temperature by 6.48°C, where the Comsol's result is about 7.2°C. The results are summarized in Table 4.1. Guillaume concluded that the accuracy of the Comsol model is acceptable. Hence, since the EES model gives better results which have lower relative deviations than the Comsol, then the EES model is acceptable as well.
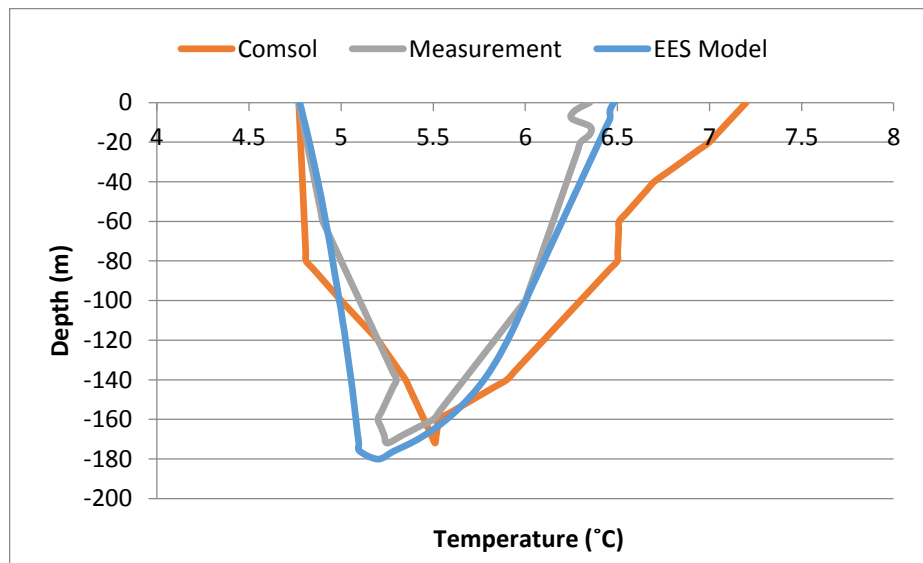
Figure 4.3. Temperature distribution between measurement, Comsol, and the EES model.
(Working fluid: water, flow rate: 2.1 kg/s)

Table 4.1. Summary of the comparing results between measurement, Comsol, and the
EES model.

	Tin (˚C)	Tout (˚C)	Relative deviation of temperature distribution (%)	
			Flow down	Flow up
Measurement	4.77	6.35		
COMSOL	4.77	7.2	1.89	5.56
EES Model	4.77	6.48	1.98	1.23

4.2   Parametric Study

As the model is validated, a parametric study is taken for constant and linear well profiles. Then, the effects of insulation, temperature gradient and depth of the well, DHE geometry, mass flow rate, and type of working fluids are investigated. Over 300 simulations have been conducted to the Thesis (see Table 4.2).

Table 4.2. The number of the simulations.

Parameters	Range	Interval	Number of Simulations
Insulation Thickness (m)	0.002-0.012	0.004	10
Pipe Material, k (W/m.K)	4-231		4
Gradient Temperature (˚C)	2-5	0.5	59
Depth (m)	1000-2000	500	53
Diameter (m)	0.1016-0.1524	0.0254	18
Flowrate (kg/s)	15-80	5	60
Working fluids	5 working fluids		63
Cases	6 cases		66
Total			333

4.2.1 Effect of Insulation Thickness, Pipe Materials, and Flow Direction of Geothermal Fluid

To avoid the heat loss of the working fluid in the inner pipe to the surrounding pipe, the inner pipe should be insulated (see Figure 3.1). The material and specification of insulation material have been given in section 3.1. The insulation is installed at any location where the temperature of the annular pipe is lower than the temperature inside the inner pipe.

The effects of insulation on the temperature distribution along 2500 m DHE are illustrated in Figure 4.4. The Figure 4.4 indicates that the insulation recommended to install start from the bottom of the inner pipe, since the temperature of the annular pipe is lower than the temperature inside the inner pipe by 148.4°C and 153.4°C, respectively.
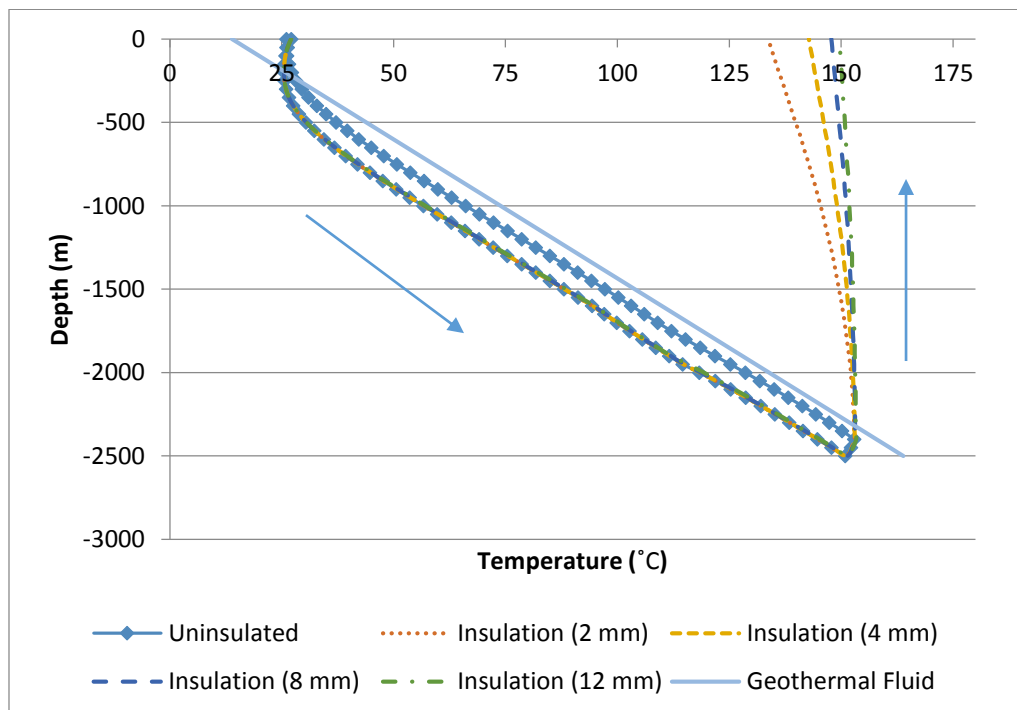
Figure 4.4. Effect of insulation to the temperature distribution of the DHE.
(Working fluid: R134a, ṁ: 30 kg/s, ΔT: 3°C/50 m)

The critical insulation thickness is about 8 mm. The increment of h will decrease the thickness of the insulation. As seen from the Figure 4.4, temperature output of the DHE without insulation is significantly decreased to 26.34°C at the surface. However,

when the DHE is insulated, the temperature output can be kept at 133.7℃ for 0.2 mm insulation thickness and the temperature output increases by adding more insulation thickness.

Moreover, insulation is desirable to maintain pressure output, since the density of working fluid is proportional to pressure drop along the channel. Figure 4.5 shows effects of insulation to pressure distribution, where without insulation pressure drop along inner pipe channel is very high due to increasing the density, whereas the density of working fluid is a function of temperature and pressure. Hence, the DHE performance is strongly affected by the insulation.
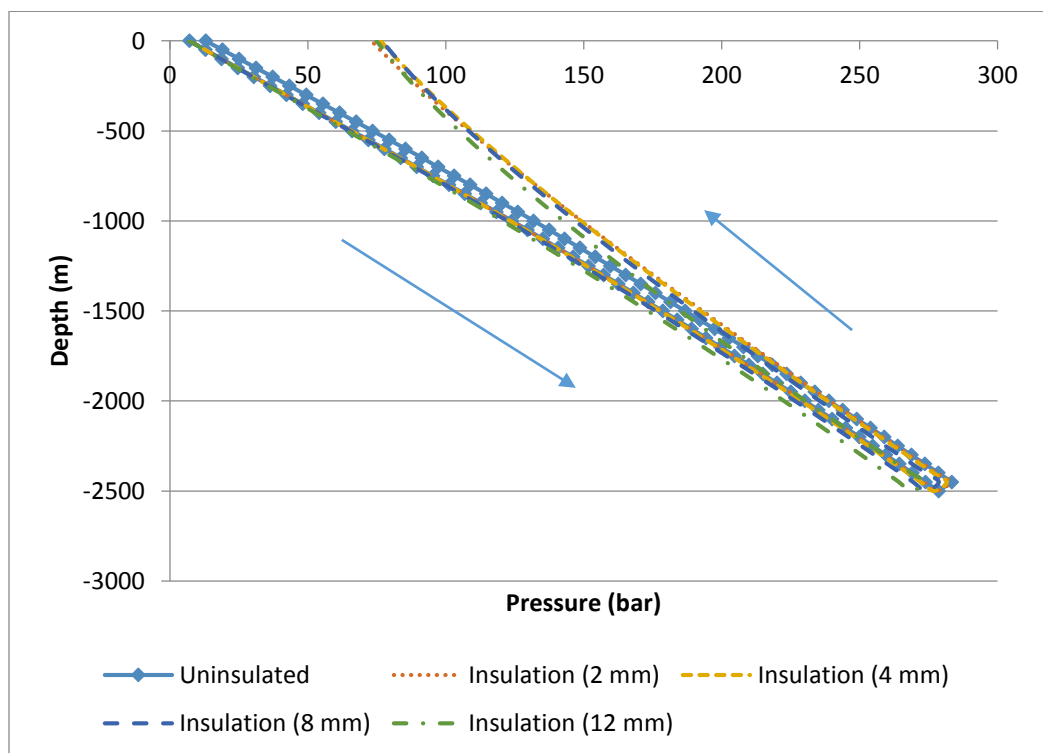
Figure 4.5. Effect of insulation to the pressure distribution of the DHE.
(Working fluid: R134a, ṁ: 30 kg/s, ΔT: 3℃/50 m)

Nonetheless, adding more thickness of insulation on the inner pipe will decrease the volume area in the annular region, which means mainly affected to mass flow rate of working fluid (Figure 4.6). Since the mass flow rate is a desirable parameter in DHE design, then an insulation thickness with relatively minimum heat loss and high flow rate must be selected. Therefore, 8 mm insulation thickness is installed for the next analyses due to that reason.
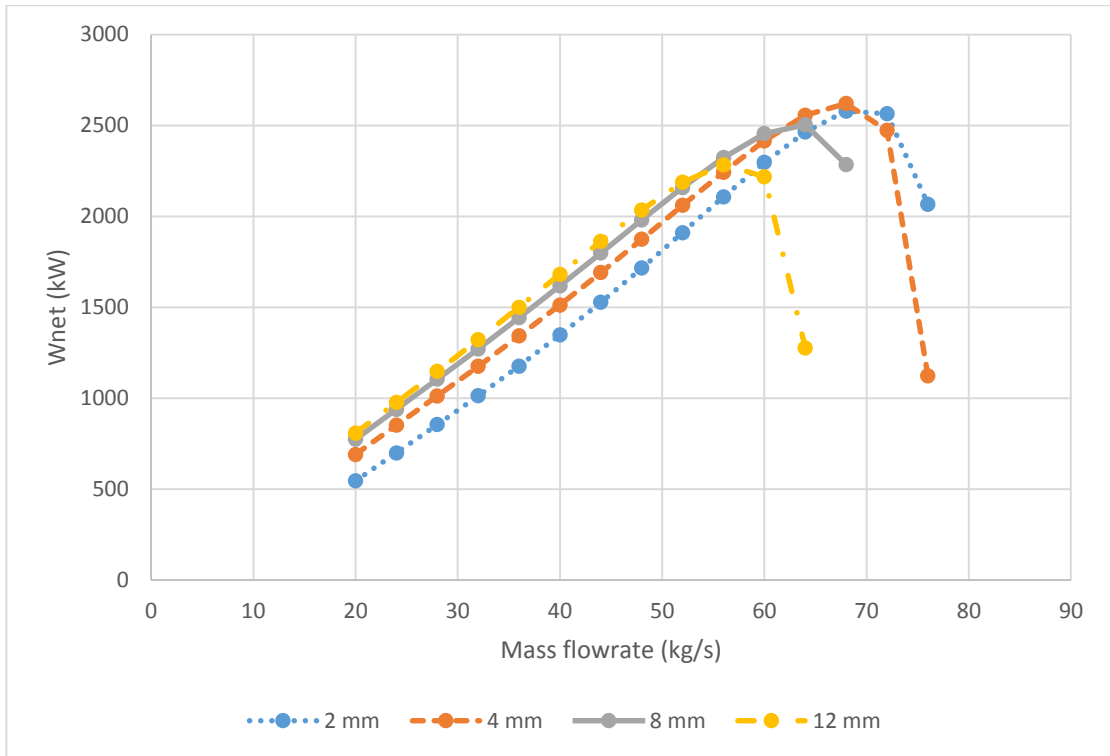
Figure 4.6. Effect of insulation thickness to the mass flow rate of working fluids.
(Working fluid: R134a, ṁ: 30 kg/s, ΔT: 3°C/50 m)

In order to see the effects of pipe materials, the DHE is calculated for different pipe materials (Figure 4.7). Table 4.3 is thermal and mechanical properties of different materials.

Table 4.3. Thermal and mechanical properties of different pipe materials.

Properties	PE-100	CS-A53	AA-2024	A-1050
k (W/m.K)	4	51	120	231
$T_{melting}$(°C)	115-137	1425- 1540	463-671	660
TS (MPa)	25	413	468	105
Roughness no.	3E-06	4.5E-05	1.5E-06	1.5E-06
Price rates	Low	Medium	High	High

Where PE: polyethylene, CS: carbon steel, AA: aluminum alloy, A: aluminum
Figure 4.7 shows the temperature profile of DHE increases with the increasing thermal conductivity of pipe materials. However, different thermal conductivity for metal

pipe materials (k > 51 W/m.K) give a slightly different. Moreover, it is relevant to the previous study that concluded heat output does not change effectively from a certain value of thermal conductivity of pipe material > 20W/mK (Alpay, 2002).
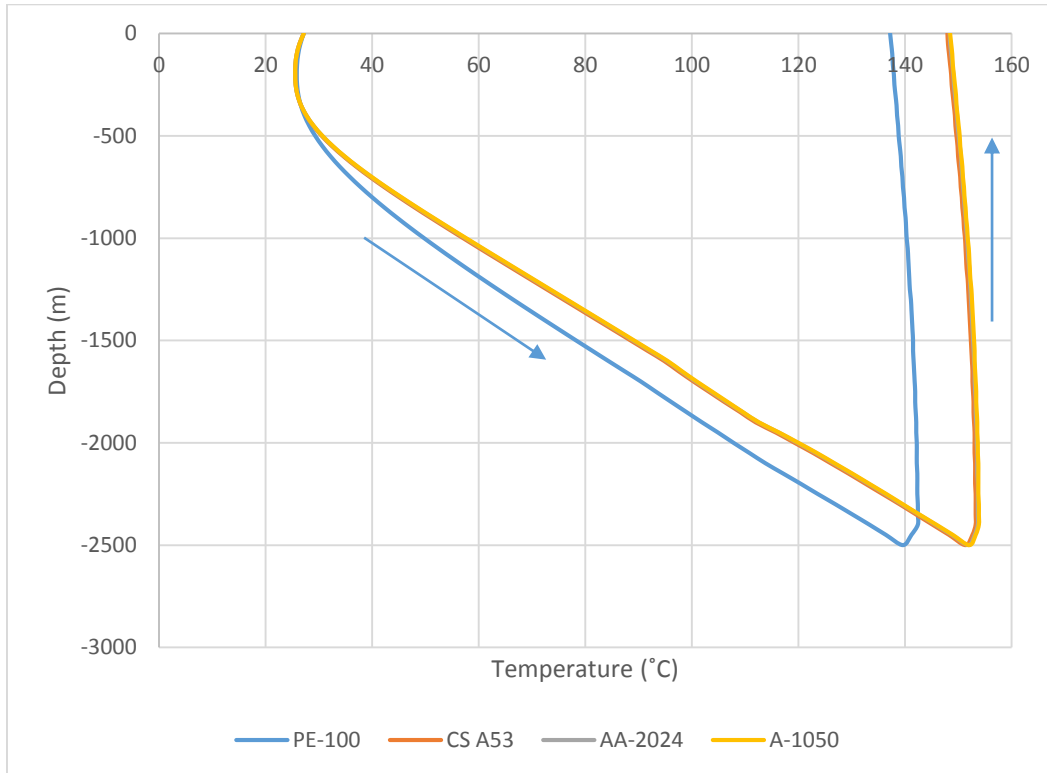
Figure 4.7. Effect thermal conductivity of pipe materials to the temperature profile of DHE.
(Working fluid: R134a, ṁ: 30 kg/s, ΔT: 3°C/50 m)

Figure 4.8 shows the pressure distribution of DHE increases with decreasing the roughness number of pipe material since the pressure drop due to friction is affected by roughness number of the pipe material.

By considering the thermal-mechanical properties and thermodynamic performance, metal pipe materials are recommended to be applied to the DHE, since the reservoir at the bottom has high temperature and pressure. For the next analyses, carbon steel pipe material is applied to the DHE.
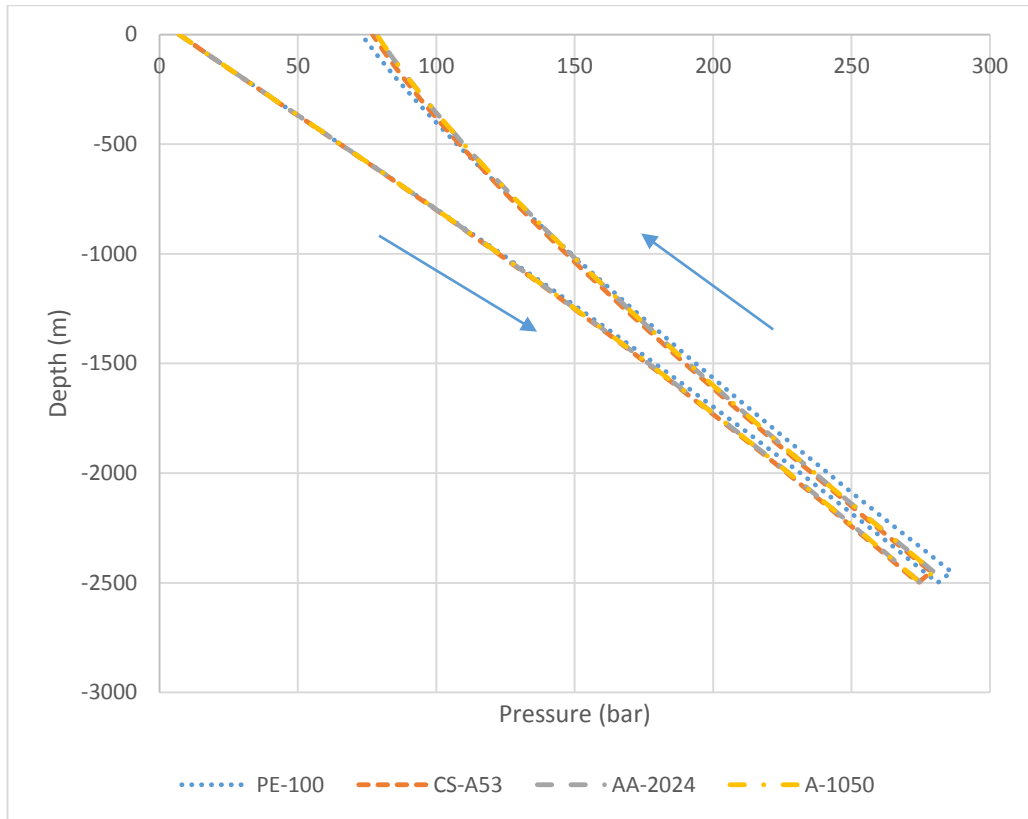
Figure 4.8. Effect roughness number of pipe materials to pressure distribution of DHE.
(Working fluid: R134a, ṁ: 30 kg/s, ΔT: 3°C/50 m)

The flow direction of the fluids on surrounding of the heat exchanger is being used to design the type of heat exchanger by using NTU method. There are two possibilities of the flow direction in the geothermal fluid. The parallel flow occurs when the direction of geothermal fluid has the same direction with the flow in the annular pipe and vice versa for the counter flow. The Figure 4.9 shows that there are no much different temperature distribution between parallel and counter flow.
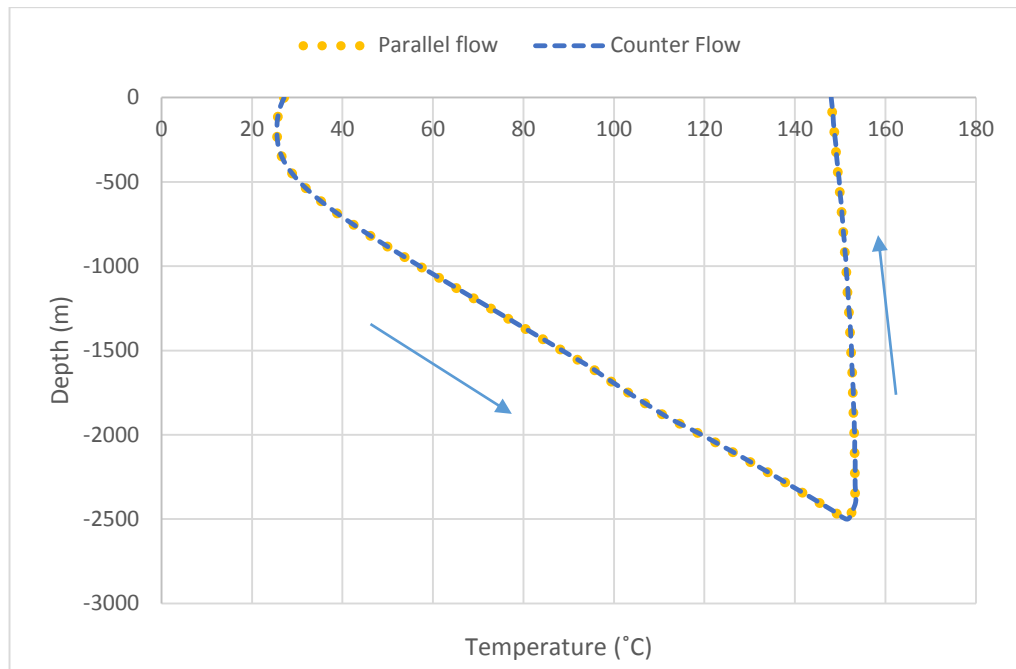
Figure 4.9. Effect of flow direction to the temperature distribution of the DHE.
(Working fluid: R134a, ṁ: 30 kg/s, ΔT: 3°C/50 m)

4.2.2 Effect of Temperature Gradient and Depth of DHE

The effect of the temperature gradient of geothermal water and depth is analyzed based on the net work output of the plant. As it can be observed from Figure 4.10, the net work output of DHE with 30 kg/s of R134a working fluid increases with increasing temperature and depth. As an example, at 4°C per 50 m of the temperature gradient, the net work output of the turbine increases approximately 37% by adding 500 m depth of DHE. Because the temperature of geothermal water at the bottom linearly increases, that means it increases the temperature and pressure of turbine inlet.

Furthermore, low-temperature gradients (below 3°C/50 m) are not recommended to be applied the DHE, since the energy desired output is less than the energy required output. Hence, the suggested temperature gradients to be applied to the DHE are higher than 3°C/50 or by enlarging the depth of the DHE over 2000 m.
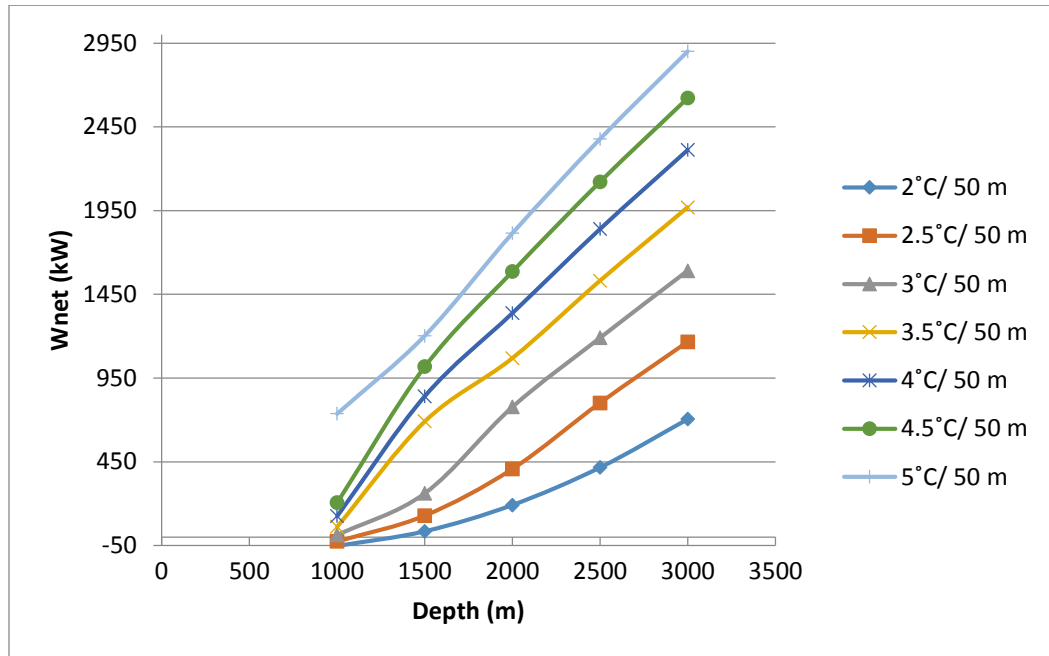
Figure 4.10. Effect of the temperature gradient of geothermal water and depth of DHE
to the net work output.
(Working fluid: R134a, ṁ: 30 kg/s)

4.2.3 Optimum Geometry and Mass Flow Rate

The DHE consists of two vertical pipes that share volume for flowing the working fluid. The increment in the diameter of the inner pipe is nearly linear to decreasing the overall heat transfer coefficient (Figure 4.11). Since the overall heat transfer coefficient is useful to define the heat exchanger thermal effectiveness and temperature output, the smaller inner pipe diameter will be maximizing the net work before the stream of working fluids will be strangled as it flows up through the inner pipe, which means increasing the pressure drop.

Figure 4.10 shows that the effect of the geometry on the overall heat transfer coefficient is valid for all type of working fluids at 2500 m depth of DHE and 12 kg/s of working fluids.
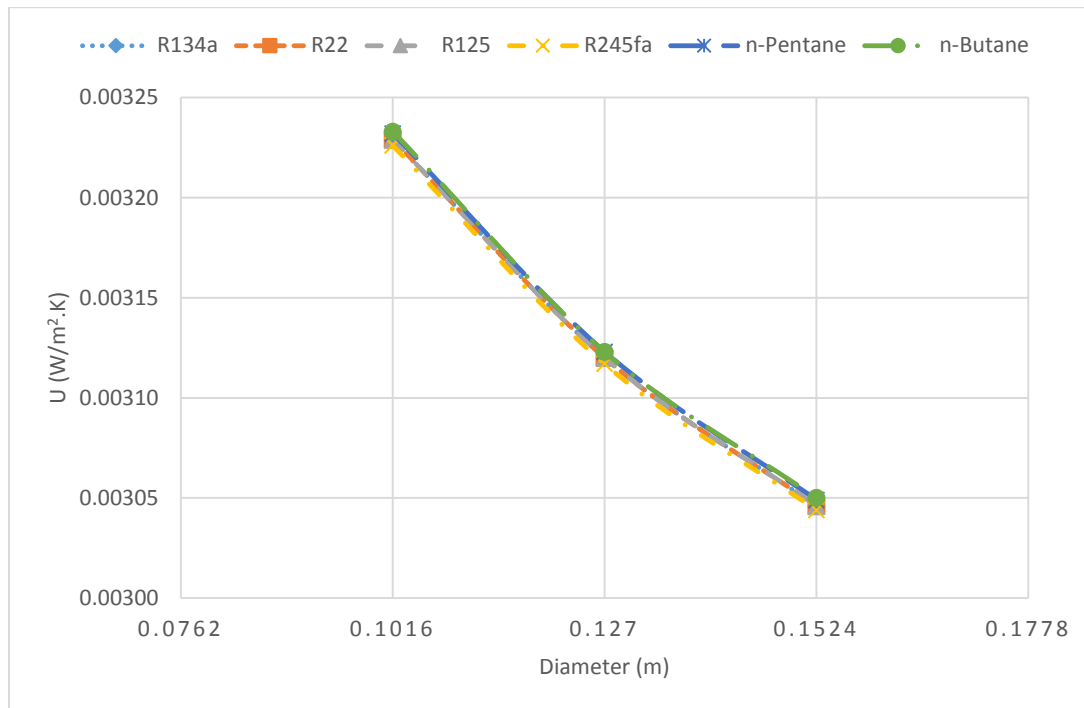
Figure 4.11. Effect of different inner pipe diameter to the overall heat transfer coefficient.
(Depth: 2500 m, ṁ: 12 kg/s, ΔT: 3ºC/50 m)

Furthermore, increasing or decreasing the inner pipe diameter is possible to give negative effect, especially to pressure drop due to friction in the channel. Figure 4.12 (a) shows that changing diameter is not significantly affect to temperature distribution along the DHE, but for a larger diameter of inner pipe (0.1524 m) reduces cross section area in the annular region that creates more frictional pressure losses (Figure 4.12 (b)). In contrast, for a smaller diameter frictional pressure losses in the annular region can be minimum, then increases when the flow goes up through the inner pipe. Hence, it is necessary to achieve the optimum diameter. In the model, the optimal diameter can be achieved by 0.127 m diameter of inner pipe since gives relatively minimum pressure losses.
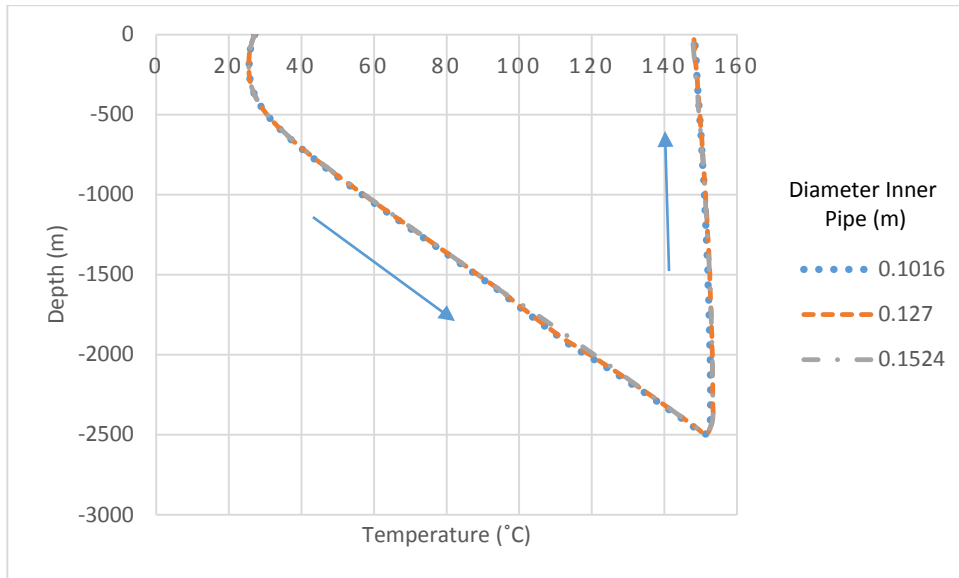
(a)
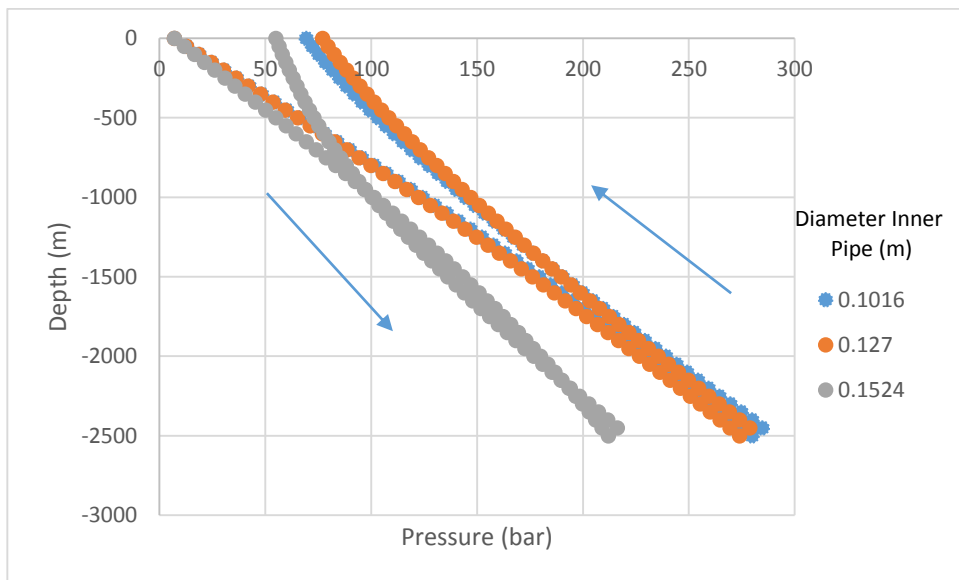
(b)

Figure 4.12. Effect of the geometry to the temperature (a) and pressure distribution (b).
(Depth: 2500 m, ṁ: 12 kg/s, ΔT: 3°C/50 m)

The heat production of the system depends on the amount of heat that can be transferred by working fluid from the ground to the surface through the DHE. Geothermal source temperature in the reservoir is obviously desirable, but since there is no sufficient mass flow rate of working fluid, the heat could not be extracted optimally. Nonetheless, increasing the mass flow rate increases pressure drop and reducing temperature output. Consequently, the optimal mass flow rate must be selected to produce a maximum net work output.

Figure 4.13 shows how the flow rate of working fluid affects the net work output. The highest net work out can be achieved by given the optimum flow rate. In another hand, the smaller inner pipe diameter needs a low flow rate to prevent the high-pressure drop of the upward stream in the inner pipe region. Which means, the mass flow rate is a significant parameter in designing of the system components.

Figure 4.13 indicates that the optimum inner pipe diameter of DHE is the inner pipe with diameter 0.127 m which gives highest net work output 2511 kW at optimum mass flow rate 64 kg/s.
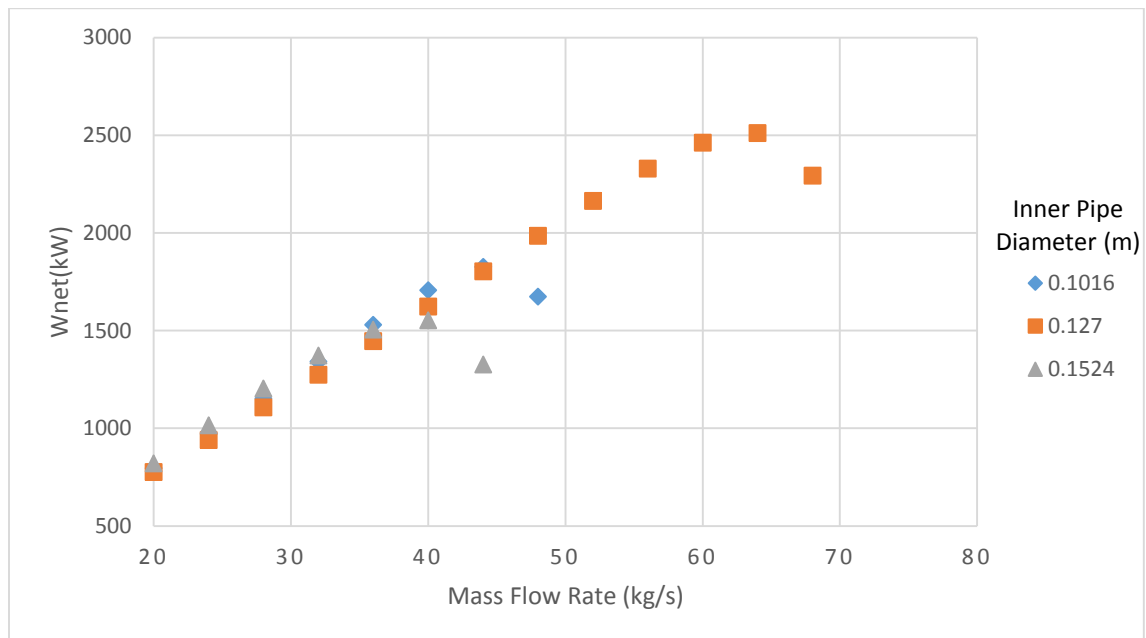
Figure 4.13. Effect of mass flow rate to work output.
(Working fluid: R134a, depth: 2500 m, ΔT: 3°C/50 m)

4.2.4 Working Fluid Selection

The selection of working fluids is evaluated based on the power generation, thermal efficiency and safety and environmental criteria. An amount of the net work out shows the performance of the working fluid on transferring thermal energy from the ground heat source to useful power generation.

Figure 4.14 shows that the refrigerant working fluids can be operating in higher flow rate level than the hydrocarbon working fluids for a specific geometry of DHE.

Which means, give a higher net work output since work is proportional to the mass flow rate. The refrigerant R134a gives the highest net work out (2511 kW) at optimum mass flow rate 64 kg/s while other working fluids show lower net work out. In another hand, the Figure 4.13 shows that the hydrocarbon working fluids give better performance when the cycle is set at a low flow rate (with net work out 2060 kW at 26 kg/s mass flow rate for n-Butane working fluid).

Thermal efficiency shows the performance of the cycle that can be assessed by the First Law of thermodynamics. Figure 4.15 illustrates the thermal efficiency of working fluids by increasing the mass flow rate. The thermal efficiency decreases for all working fluids by increasing mass flow rate. The reduction in flow rate is a result of the improved cycle efficiency with a high source temperature. There are three working fluids (R134a, R22, and n-Butane) that show a better performance regarding thermal efficiency (over 19%) while other working fluids show much lower thermal efficiency.
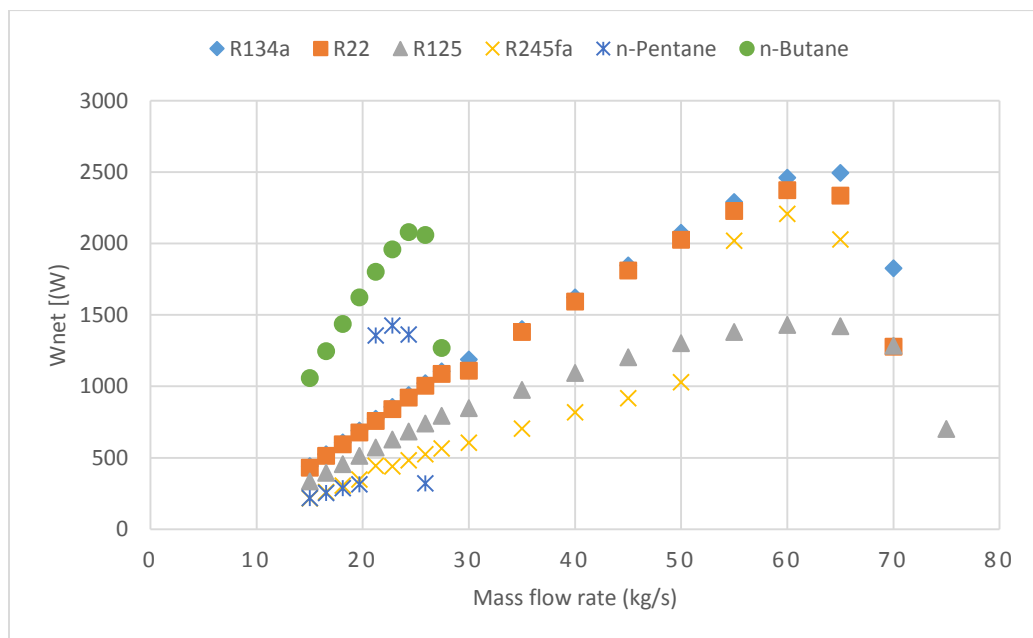
Figure 4.14. The net work out for some different working fluids.
(Depth: 2500 m, ΔT: 3°C/50 m, Dt: 0.127 m)
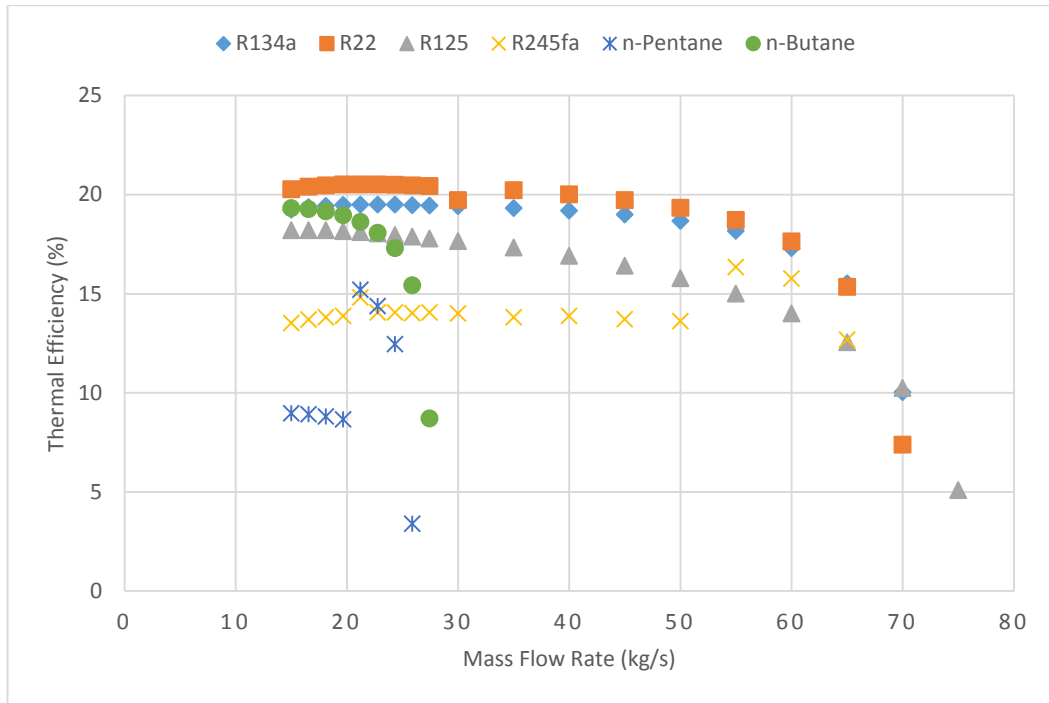
Figure 4.15. The thermal efficiency versus mass flowrate.
(Depth: 2500 m, ΔT: 3°C/50 m, Dt: 0.127 m)

Besides the thermodynamic performances, the safety and environmental criteria also should be considered in the selection of working fluids. The safety and environmental criteria are key of importance in working fluid selection since not all of working fluids are environmentally friendly. Some of working fluids have good thermodynamic performance but at the same time they are very flammable fluid and have undesirable environmental effects.

Table 4.4 gives safety and environmental data for selected working fluids. In term of the environmental data (number of ozone depletion potential (ODP) and global warming potential (GWP) hydrocarbon fluids are more environmentally friendly than the refrigerant working fluids but at the same time, they are very flammable. In many countries, some of working fluids are already forbidden due to their ODP and GWP numbers.

Table 4.4. Safety and environmental data of selected working fluids.
(Source: Acuña, 2010)

| Working Fluid | Physical Data | | | Safety Data | | | Environmental Data | | | | Expansion |
	NBP (°C)	TC (°C)	PC (kPa)	OEL (ppMv)	LFL	Safety	Atm. Life time	ODP	GWP (100 yr)	
R134a	-26	101	40.59			A1	14.6	0	1300	wet
R22	-40.8	96.1	49.9	1000		A1	11.9	0.04	1790	wet
R125	-48.1	66	36.18	1000		A1	32.6	0	2800	wet
R245fa	15.14	154	36.51	300		B1	7.7	0	1050	dry
n-Pentane	36.1	196.55	33.7	600	1.2	A3	0.009	0	20	dry
n-Butane	-6.31	146.14	40.05	1000	1.8	A3				dry

4.3   Economic Analysis

In this section, DHE power generation system are evaluated based on SPT, cost electricity production rate (CEP), and NPV. The economical analyses are given based on six geometry optimization cases (Table 4.5). Case 1-3 are the DHEs with different diameter of the inner pipe but have the same depth, whereas case 4-6 are the DHEs with the same diameter of inner pipe but have different depth.

Changing the geometry of the DHE gives different work output and costs, which is desirable to understand when a new DHE system is being built. In the calculation, economical parameters and assumptions are described in section 3.3 from the Chapter 3 for the electricity sales price of 0.105 $/kWh. The cash flow of plant is calculated for 20 years economical life with a stable interest rate at 10%.

Table 4.5. Selected the highest net work output for six different cases.

Name of Cases		Wnet (kW)					
		Case 1	Case 2	Case 3	Case 4	Case 5	Case 6
Diameter (m)		0.1016	0.127	0.1524	0.127		
Depth (m)		2500			2000	2500	3000
Mass Flowrate (kg/s)	20	796.2	775.3	820.9	494.5	775.3	1042
	24	971.6	940.4	1015	600.8	940.4	1263
	28	1153	1107	1204	715.2	1107	1482
	32	1341	1274	1373	839.1	1274	1700
	36	1530	1447	1505	986.5	1447	1916
	40	1707	1623	1552	1148	1623	2132
	44	1827	1804	1326	1311	1804	2345
	48	1674	1986		1466	1986	2555
	52		2164		1607	2164	2756
	56		2330		1717	2330	2941
	60		2462		1754	2462	3089
	64		2511		1584	2511	3152
	68		2294		74.78	2294	2960

The general results of the economical evaluation of DHE power generation are given in Table 4.6. The table shows that more work production gives total investment and operational costs more. The best design is given by case study 6 (3000 m of depth with 0.127 inner pipe diameter) which gives the largest net revenue ($1.75 millions) and much faster payback time at 2.24 years. The cost electricity production rates are nearly equal for all case studies at 46 $/MWh, which means in the range of average cost electricity production rate of the geothermal source with a range of 43.8 - 52.1 $/MWh (EIA, 2015).

Table 4.6. General results of economical evaluation of DHE power generation.

	Unit	Case 1	Case 2	Case 3	Case 4	Case 5	Case 6
Electric work Output	(kW)	1827	2511	1552	1754	2511	3152
Annual Electricity Production	(GWh)	15.20	20.89	12.91	14.59	20.89	26.23
Total Investment	(million $)	2.31	3.14	2.01	2.21	3.14	3.94
O & M Cost	(million $)	0.57	0.79	0.49	0.55	0.79	0.99
Electricity Sales Revenue	(million $)	1.59	2.19	1.35	1.53	2..19	2.75
Net Revenue	(million $)	1.01	1.40	0.86	0.97	1.40	1.75
Simple Payback Time	(year)	2.27	2.25	2.32	2.26	2.25	2.24
Cost Electricity Production	($/kWh)	0.046	0.046	0.046	0.046	0.046	0.046

4.3.1 Net Present Value

This evaluation takes electricity sales price range of 0.055-0.105 $/kWh and 10% interest rate. The NPV linearly increases by increasing the sales price. Figure 4.16 shows that a negative NPV of sales price 0.055 $/kWh for all of the cases. Which means, the DHE is not a good investment for low electricity sales price. However, when the sales price increases to more than 0.065 $/kWh, all cases give positive NPV.

Figure 4.16. NPV of the DHE power generation versus electricity sales price rates.

4.4 Summary of the Results

4.4.1 Thermodynamic Analysis

- Insulation is highly recommended to be installed on the DHE system. Because it gives a positive performance to the DHE, especially increasing the temperature output by decreasing the heat loss.
- The insulation is recommended to be installed at any location where the temperature of the annular pipe is lower than the temperature inside the inner pipe.
- To improve the performance of the DHE, the application of higher temperature gradient and deeper of depth is very useful.
- A suggested temperature gradient is the temperature gradient with more than 3°C/50 m.
- At a low mass flow rate, the smaller diameter of inner pipe gives better performance than the larger diameter. The overall heat transfer coefficient decreases by increasing the diameter of the inner pipe.
- To maximize the net work output, the optimum of diameter and mass flow rate are should be achieved.

- At a low mass flow rate, the hydrocarbon working fluids give better performance than the refrigerant working fluids.
- Regarding the highest number of net work output that can be produced by the DHE, using refrigerant R134a is very recommended. Because, it gives 2511 kW for a single well (for design depth: 2500 m, ΔT: 3°C/L, Dt: 0.127).
- Besides having better thermal efficiency, the refrigerant working fluids also have a better safety compare to the hydrocarbons which are very flammable.

4.4.2 Economic Analysis

- According to the net revenue, SPT, and NPV evaluation, the Case 6 (depth: 3000 m, Dt: 0.127) gives the best design of the DHE. Which means, larger net work output relatively gives better performance in term of economic analysis. Consequently, the engineer should design the DHE with deeper of depth and larger of DHE system for a large amount of working fluid.
- The cost electricity production of the DHE power generation is about 46 $/MWh, which is much cheaper than the conventional geothermal power generation.
- According to the NPV evaluation, an investment on the DHE power generation is not recommended when the electricity sales price lower than 0.065 $/kWh.

CHAPTER 5

CONCLUSIONS AND FUTURE STUDIES

5.1 Conclusions

In this Thesis, the DHE system has been developed by EES software to examine the thermodynamic and economic feasibility for power generation. The model is simulated based on depth and temperature gradient of geothermal heat source, the diameter of the inner pipe, mass flowrate and type of working fluids. The model has been simulated through over 300 simulations to achieve the best design regarding thermodynamic and economic evaluation.

The analyses indicate that the characteristics of geothermal heat source, the geometry of DHE, optimum mass flowrate, and type of working fluids are desirable parameters when a new system is being built. Based on the maximum obtainable net work output that can be produced by GPP with DHE, using refrigerant R134a is highly recommended with a net work output of 2511 kW for a single well (for design depth: 2500 m, ΔT: 3°C/L, Dt: 0.127 m, ṁ: 64 kg/s). The optimum mass flowrate that gives maximum work output can be achieved depends on the type of working fluids and the geometry of the DHE.

The best design of the DHE obtained under the conditions of Case 6 which gives a net work output of 3152 kW with annual net revenue and payback time are $1.75 million and 2.24 years, respectively.

According to the NPV evaluation, the DHE power generation gives positive value when the electricity sales price is 0.065 $/kWh or higher, which means an investment in the DHE power generation is acceptable.

Finally, according to the thermodynamic and economic evaluation, the analyses concluded that the DHE system is feasible for an alternative power generation.

5.2 Future Studies

- A DHE design with a promoter pipe in the well is suggested for future study to give a better performance of DHE.
- A transient study should be developed in the future studies to examine the sustainability of geothermal heat source and cycle performance along a year.

REFERENCES

Acuña, J. (2010). *Improvements of U-pipe borehole heat exchangers.* (Licentiate Thesis), KTH School of Industrial Engineering and Management, Stockholm, Sweden.

Akhmadullin, I., & Tyagi, M. (2014). Design and Analysis of Electric Power Production Unit for Low Enthalpy Geothermal Reservoir Applications. *World Academy of Science, Engineering and Technology, International Journal of Environmental, Chemical, Ecological, Geological and Geophysical Engineering, 8*(6), 443-449.

Alpay, S. (2002). Numerical analysis of finned downhole heat exchangers: A parametric study.

Anh, L. N. (2009). *Thermodynamic data of working fluids for energy engineering.* (Ph.D Thesis), University of Natural Resources, Vienna, Austria.

Bahrami, M., Hamidi, A. A., & Porkhial, S. (2013). Investigation of the effect of organic working fluids on thermodynamic performance of combined cycle Stirling-ORC. *International Journal of Energy and Environmental Engineering, 4*(1), 1-9.

Baik, Y.-J., Kim, M., Chang, K. C., & Kim, S. J. (2011). Power-based performance comparison between carbon dioxide and R125 transcritical cycles for a low grade heat source. *Applied Energy, 88*(3), 892-898.

Boyle, G. (1996). *Renewable Energy: Power for a Sustainable*: Oxford University Press, USA.

Brown, D. W., Duchane, D. V., Heiken, G., & Hriscu, V. T. (2012). The Enormous Potential for Hot Dry Rock Geothermal Energy *Mining the Earth's Heat: Hot Dry Rock Geothermal Energy* (pp. 17-40): Springer.

Cengel, Y. (2007). *Introduction to thermodynamics and heat transfer+ EES software*: New York: McGraw Hill Higher Education Press.

Culver, G., & Lund, J. W. (1999). Downhole heat exchangers. *Geo-Heat Center Quarterly Bulletin, 20*(3).

Culver, G. G., & Reistad, G. M. (1978). *Testing and modeling of downhole heat exchangers in shallow geothermal systems*. Retrieved from USA:

DiPippo, R. (2012). *Geothermal power plants: principles, applications, case studies and environmental impact*: Butterworth-Heinemann, USA.

Domínguez Masalias, M. (2010). *Thermodynamic optimization of downhole coaxial heat exchanger for geothermal applications.* (Master Thesis), Warsaw University of Technology, Poland.

Duchane, D., & Brown, D. (2002). Hot dry rock (HDR) geothermal energy research and development at Fenton Hill, New Mexico. *Geo-Heat Center Bulletin, 23*(4), 13-19.

EIA. (2015). *Levelized Avoided Cost of New Generation Resources in the Annual Energy Outlook 2015*. Retrieved from USA:

Elíasson, L., & Valdimarsson, P. (2005). *Economic Evaluation of power production from a geothermal reservoir.* Paper presented at the Proceedings World Geothermal Congress, Antalya, Turkey.

Feng, Y. (2012). *Numerical study of downhole heat exchanger concept in geothermal energy extraction from saturated and fractured reservoirs.* (Ph.D Thesis), University of Louisiana, Lafayette, USA.

GEA. (2015). Annual US & global geothermal power production report. *Washington DC, USA*.

Guillaume, F. (2011). *Analysis of a novel pipe in pipe coaxial borehole heat exchanger.* (Master Thesis), KTH School of Industrial Engineering and Management, Stockholm, Sweden.

Hance, C. N. (2005). Factors affecting costs of geothermal power development. *Geothermal Energy Association for the US Department of Energy*.

Hatboru. (2016). *Carbon Steel Price lists*. www.hatboru.com

Kakac, S., Liu, H., & Pramuanjaroenkij, A. (2012). *Heat exchangers: selection, rating, and thermal design*: CRC press.

Kakaç, S., Shah, R. K., & Aung, W. (1987). *Handbook of single-phase convective heat transfer*: Wiley New York et al.

Kalra, C., Becquin, G., Jackson, J., Laursen, A. L., Chen, H., Myers, K., . . . Zia, J. (2012). *High-Potential Working Fluids and Cycle Concepts for Next-Generation Binary Organic Rankine Cycle for Enhanced Geothermal Systems.* Paper presented at the 37th Workshop on Geothermal Reservoir Engineering, Stanford, CA, USA.

Karadas, M. (2016). HD Energy Consultancy co. Inc. Turkey.

Kilicarslan, A., & Müller, N. (2005). A comparative study of water as a refrigerant with some current refrigerants. *International journal of energy research, 29*(11), 947-959.

Konyalı, A. (2010). *Financial Evaluation of Kizildare Geothermal Power Plant.* (Master Thesis), Izmir Institute of Technology, Izmir, Turkey.

Lei, H., Liu, X., & Dai, C. (2012). Experiment of Heat Transfer in Downhole Heat Exchangers With a Promoter Pipe. *GRC Transactions, Vol. 36*.

Lund, J. W. (1999). Large downhole heat exchanger in Turkey and Oregon. *Geo-Heat Center Quarterly Bulletin, 20*(3).

Lund, J. W. (2010). Direct utilization of geothermal energy. *Energies, 3*(8), 1443-1471.

Lund, J. W., & Boyd, T. L. (2016). Direct utilization of geothermal energy 2015 worldwide review. *Geothermics, 60*, 66-93.

Luo, J., Rohn, J., Bayer, M., & Priess, A. (2013). Thermal efficiency comparison of borehole heat exchangers with different drillhole diameters. *Energies, 6*(8), 4187-4206.

Maclaine-Cross, I., & Leonardi, E. (1997). Why hydrocarbons save energy. *AIRAH JOURNAL, 51*, 33-38.

Masheiti, S., Agnew, B., & Walker, S. (2011). An evaluation of R134a and R245fa as the working fluid in an Organic Rankine Cycle energized from a low temperature geothermal energy source. *Journal of Energy and Power Engineering, 5*(5).

Massoud, M. (2005). *Engineering thermofluids*: Springer.

Morita, K., Bollmeier, W. S., & Mizogami, H. (1992). Analysis of the results from the downhole coaxial heat exchanger (DCHE) experiment in Hawaii.

Morita, K., & Ogawa, M. (1998). Geothermal and solar heat used to melt snow on roads. *GRC Bulletin, 26*(3), 83-85.

Morita, K., Tago, M., & Ehara, S. (2005). *Case studies on small-scale power generation with the downhole coaxial heat exchanger.* Paper presented at the Proc. World Geothermal Congress, Antalya, Turkey.

Nalla, G., Shook, G. M., Mines, G. L., & Bloomfield, K. K. (2005). Parametric sensitivity study of operating and design variables in wellbore heat exchangers. *Geothermics, 34*(3), 330-346.

Pan, H., Freeston, D., & Lienau, P. (1982). *Experimental performance of downhole heat exchangers—model and full scale.* Paper presented at the Proc. Pacific Geother. Conf.

Redko, A., Kulikova, N., Pavlovsky, S., Bugai, V., & Redko, O. (2016). *Efficiency of Geothermal Power Plant Cycles with Different Heat-Carriers.* Paper presented at the Workshop on Geothermal Reservoir Engineering, Stanford University, California, USA.

Şener, A. C., & Uluca, B. (2009). *Türkiye Elektrik Piyasalari ve Jeotermal Enerjinin Konumu.* Paper presented at the Jeotermal Enerji Semineri Kitabi, TESKON, , Turkey.

Tola, V., & Finkenrath, M. (2015). Performance evaluation of an Organic Rankine Cycle fed by waste heat recovered from CO2 capture section. *International Journal of Thermodynamics, 18*(4), 225-233.

Wang, Z., McClure, M. W., & Horne, R. N. (2010). *Modeling study of single-well EGS configurations.* Paper presented at the Proceedings World Geothermal Congress, Bali, Indonesia.

APPENDIX A

THERMODYNAMIC PROPERTIES OF SELECTED WORKING FLUID

Working Fluids	NBP [K]	Critical Temperature ([K])	Critical Pressure [kPa]	Density [kg/m3]	Heat of Vaporization [kJ/kg]	Atm life time	ODP	GWP	Safety
R134a	247	374	4059	4.258	217	14.6	0	1300	A1
R245fa	288.14	427	3651	5.718	196		0	1050	B1
R22	238.2	369.1	4990	1186	205.1	11.9	0.04	1790	A1
R125	230.9	339	3618	573.58		32.6	0	2800	A1
n-Pentane	36.1	196.5	3364	620.8	358	0.009	0	20	A3
n-Butane	272.69	419.14	4005	602	365				A3

APPENDIX B

AN EXAMPLE FOR DHE CALCULATION BY USING EES SOFTWARE

L (m)	T_{geo} (^oC)	T_h (^oC)	T_c (^oC)	ρ (kg/m^3)	Pr	Re	Nu	h_f ($W/m^2.K$)	Gr	Pr	Ra	Nu_w	h_w ($W/m^2.K$)	U ($W/m^2.K$)	q (kW)	ε	NTU	T_i (^oC)	P_i (bar)
0	13.89	15.39	21.25	1199	3.38	4.81E+06	14112	14.41	8.87E+14	8.16	7.2E+15	48250	0.082	8.6E-02	-33.9	3.2E-02	3.3E-02	27.1	7.1
-50	16.89	18.39	22.57	1203	3.35	4.83E+06	14135	14.43	8.98E+14	7.48	6.7E+15	47279	0.080	8.4E-02	-23.7	3.1E-02	3.2E-02	26.7	12.3
-100	19.89	21.39	23.93	1208	3.33	4.87E+06	14193	14.46	7.39E+14	6.89	5.1E+15	42691	0.072	7.6E-02	-13.1	2.9E-02	2.9E-02	26.5	17.6
-150	22.89	24.39	25.36	1211	3.31	4.91E+06	14256	14.5	3.68E+14	6.36	2.3E+15	31556	0.053	5.7E-02	-3.7	2.1E-02	2.2E-02	26.3	22.9
-200	25.89	27.39	26.84	1214	3.29	4.95E+06	14325	14.54	2.64E+14	5.90	1.6E+15	26986	0.046	4.8E-02	1.8	1.8E-02	1.9E-02	26.3	28.2
-250	28.89	30.39	28.35	1217	3.27	5.00E+06	14397	14.58	1.22E+15	5.48	6.7E+15	48706	0.082	8.6E-02	11.8	3.2E-02	3.3E-02	26.3	33.5
-300	31.89	33.39	29.92	1220	3.25	5.05E+06	14474	14.62	2.54E+15	5.11	1.3E+16	63956	0.108	1.1E-01	25.9	4.1E-02	4.3E-02	26.4	38.8
-350	34.89	36.39	31.56	1221	3.23	5.10E+06	14559	14.67	4.27E+15	4.78	2.0E+16	77049	0.129	1.3E-01	42.7	4.9E-02	5.1E-02	26.7	44.2
-400	37.89	39.39	33.3	1223	3.20	5.15E+06	14656	14.72	6.42E+15	4.48	2.9E+16	88914	0.149	1.5E-01	61.2	5.6E-02	5.8E-02	27.2	49.5
-450	40.89	42.39	35.14	1223	3.18	5.22E+06	14764	14.77	9.03E+15	4.21	3.8E+16	99909	0.167	1.7E-01	80.6	6.1E-02	6.4E-02	27.9	54.9
-500	43.89	45.39	37.08	1223	3.16	5.28E+06	14886	14.83	1.21E+16	3.96	4.8E+16	110204	0.183	1.8E-01	100.3	6.7E-02	7.0E-02	28.8	60.3

(cont. on next page)

APPENDIX B (cont.)

-550	46.89	48.39	39.14	1222	3.13	5.36E+06	15020	14.89	1.57E+16	3.74	5.9E+16	119897	0.198	2.0E-01	119.9	7.2E-02	7.5E-02	29.9	65.6
-600	49.89	51.39	41.3	1220	3.11	5.44E+06	15167	14.96	1.97E+16	3.54	7.0E+16	129051	0.212	2.1E-01	138.8	7.6E-02	8.0E-02	31.2	71.0
-650	52.89	54.39	43.57	1217	3.08	5.53E+06	15328	15.03	2.42E+16	3.35	8.1E+16	137711	0.225	2.2E-01	156.7	8.0E-02	8.5E-02	32.8	76.4
-700	55.89	57.39	45.94	1214	3.05	5.62E+06	15500	15.1	2.92E+16	3.18	9.3E+16	145914	0.237	2.3E-01	173.4	8.3E-02	8.8E-02	34.5	81.7
-750	58.89	60.39	48.4	1210	3.03	5.72E+06	15684	15.18	3.46E+16	3.03	1.0E+17	153693	0.248	2.4E-01	188.7	8.6E-02	9.2E-02	36.4	87.0
-800	61.89	63.39	50.95	1206	3.00	5.82E+06	15879	15.26	4.05E+16	2.88	1.2E+17	161078	0.258	2.5E-01	202.7	8.9E-02	9.5E-02	38.5	92.3
-850	64.89	66.39	53.57	1201	2.98	5.93E+06	16083	15.34	4.69E+16	2.75	1.3E+17	168097	0.267	2.6E-01	215.2	9.2E-02	9.8E-02	40.8	97.6
-900	67.89	69.39	56.26	1196	2.95	6.04E+06	16296	15.42	5.37E+16	2.63	1.4E+17	174778	0.276	2.7E-01	226.3	9.4E-02	1.0E-01	43.1	102.9
-950	70.89	72.39	59.02	1190	2.92	6.16E+06	16517	15.51	6.10E+16	2.52	1.5E+17	181148	0.283	2.7E-01	236.0	9.6E-02	1.0E-01	45.6	108.1
-1000	73.89	75.39	61.83	1184	2.90	6.28E+06	16745	15.59	6.86E+16	2.41	1.7E+17	187231	0.290	2.8E-01	244.4	9.8E-02	1.1E-01	48.3	113.3
-1050	76.89	78.39	64.68	1178	2.87	6.40E+06	16979	15.67	7.67E+16	2.32	1.8E+17	193051	0.297	2.9E-01	251.7	9.9E-02	1.1E-01	51.0	118.5
-1100	79.89	81.39	67.58	1172	2.85	6.53E+06	17217	15.76	8.52E+16	2.23	1.9E+17	198632	0.303	2.9E-01	258.0	1.0E-01	1.1E-01	53.8	123.6
-1150	82.89	84.39	70.5	1165	2.82	6.66E+06	17460	15.84	9.42E+16	2.14	2.0E+17	203995	0.308	3.0E-01	263.2	1.0E-01	1.1E-01	56.6	128.7
-1200	85.89	87.39	73.46	1158	2.80	6.79E+06	17706	15.93	1.04E+17	2.06	2.1E+17	209161	0.313	3.0E-01	267.7	1.0E-01	1.1E-01	59.5	133.7
-1250	88.89	90.39	76.45	1152	2.78	6.92E+06	17954	16.01	1.13E+17	1.99	2.3E+17	214149	0.318	3.0E-01	271.4	1.0E-01	1.1E-01	62.5	138.8
-1300	91.89	93.39	79.45	1145	2.75	7.06E+06	18205	16.09	1.24E+17	1.92	2.4E+17	218975	0.322	3.1E-01	274.4	1.1E-01	1.1E-01	65.5	143.8
-1350	94.89	96.39	82.47	1138	2.73	7.19E+06	18456	16.17	1.34E+17	1.86	2.5E+17	223656	0.326	3.1E-01	276.9	1.1E-01	1.1E-01	68.6	148.7
-1400	97.89	99.39	85.51	1130	2.71	7.33E+06	18708	16.25	1.45E+17	1.80	2.6E+17	228207	0.330	3.2E-01	278.9	1.1E-01	1.2E-01	71.6	153.6

(cont. on next page)

APPENDIX B (cont.)

-1450	100.9	102.4	88.55	1123	2.69	7.47E+06	18959	16.32	1.57E+17	1.74	2.7E+17	232641	0.334	3.2E-01	280.5	1.1E-01	1.2E-01	74.7	158.5
-1500	103.9	105.4	91.61	1116	2.67	7.61E+06	19210	16.4	1.69E+17	1.69	2.9E+17	236970	0.337	3.2E-01	281.7	1.1E-01	1.2E-01	77.8	163.3
-1550	106.9	108.4	94.67	1109	2.65	7.74E+06	19460	16.47	1.81E+17	1.64	3.0E+17	241205	0.340	3.2E-01	282.7	1.1E-01	1.2E-01	81.0	168.1
-1600	109.9	111.4	97.73	1102	2.63	7.88E+06	19708	16.54	1.94E+17	1.59	3.1E+17	245356	0.343	3.3E-01	283.4	1.1E-01	1.2E-01	84.1	172.9
-1650	112.9	114.4	100.8	1095	2.61	8.02E+06	19954	16.61	2.07E+17	1.55	3.2E+17	249432	0.346	3.3E-01	283.9	1.1E-01	1.2E-01	87.2	177.6
-1700	115.9	117.4	103.9	1088	3.12	8.16E+06	22482	15.41	2.21E+17	1.51	3.3E+17	253440	0.289	2.8E-01	243.5	9.5E-02	1.0E-01	90.4	182.3
-1750	118.9	120.4	106.7	1082	3.10	8.28E+06	22734	15.46	2.39E+17	1.47	3.5E+17	259111	0.293	2.8E-01	249.2	9.6E-02	1.0E-01	93.1	186.9
-1800	121.9	123.4	109.6	1077	3.09	8.40E+06	22988	15.5	2.58E+17	1.43	3.7E+17	264552	0.297	2.9E-01	254.1	9.7E-02	1.0E-01	95.8	191.5
-1850	124.9	126.4	112.5	1071	3.07	8.52E+06	23243	15.55	2.77E+17	1.40	3.9E+17	269790	0.301	2.9E-01	258.3	9.8E-02	1.0E-01	98.6	196.1
-1900	127.9	129.4	115.4	1065	3.05	8.64E+06	23499	15.59	2.97E+17	1.36	4.0E+17	274848	0.304	2.9E-01	261.9	9.8E-02	1.1E-01	101.5	200.7
-1950	130.9	132.4	118.4	1059	2.29	8.77E+06	20166	17.58	3.17E+17	1.33	4.2E+17	279748	0.406	3.8E-01	333.1	1.2E-01	1.4E-01	104.4	205.2
-2000	133.9	135.4	121.7	1050	2.27	8.92E+06	20399	17.65	3.28E+17	1.30	4.3E+17	281414	0.406	3.8E-01	324.7	1.2E-01	1.4E-01	108.1	209.7
-2050	136.9	138.4	125	1042	2.26	9.06E+06	20624	17.72	3.41E+17	1.27	4.3E+17	283334	0.406	3.8E-01	317.6	1.2E-01	1.4E-01	111.7	214.1
-2100	139.9	141.4	128.3	1035	2.24	9.21E+06	20841	17.79	3.54E+17	1.25	4.4E+17	285473	0.406	3.8E-01	311.7	1.2E-01	1.4E-01	115.2	218.5
-2150	142.9	144.4	131.5	1027	2.22	9.35E+06	21051	17.85	3.68E+17	1.22	4.5E+17	287802	0.407	3.8E-01	306.8	1.2E-01	1.4E-01	118.7	222.8
-2200	145.9	147.4	134.7	1020	2.21	9.48E+06	21255	17.91	3.83E+17	1.20	4.6E+17	290296	0.408	3.8E-01	302.7	1.2E-01	1.4E-01	122.1	227.2
-2250	148.9	150.4	137.9	1013	2.19	9.61E+06	21453	17.97	3.99E+17	1.18	4.7E+17	292932	0.409	3.8E-01	299.2	1.2E-01	1.4E-01	125.4	231.4
-2300	151.9	153.4	141.1	1006	2.18	9.74E+06	21646	18.02	4.16E+17	1.15	4.8E+17	295691	0.410	3.8E-01	296.3	1.3E-01	1.4E-01	128.8	235.7

APPENDIX B (cont.)

-2350	154.9	156.4	144.2	1000	2.16	9.87E+06	21833	18.07	4.33E+17	1.13	4.9E+17	298558	0.412	3.8E-01	293.8	1.3E-01	1.4E-01	132.0	239.8
-2400	157.9	159.4	147.3	993.6	2.15	1.00E+07	22016	18.12	4.51E+17	1.11	5.0E+17	301520	0.413	3.8E-01	291.8	1.3E-01	1.4E-01	135.3	244.0
-2450	160.9	162.4	150.5	987.3	2.13	1.01E+07	22195	18.17	4.70E+17	1.09	5.1E+17	304564	0.415	3.9E-01	290.0	1.3E-01	1.4E-01	138.5	248.1
-2500	163.9	162.4	152.1	981.2	2.13	1.01E+07	12519	10.24	4.07E+17	1.09	4.5E+17	287436	0.392	3.5E-01	149.8	7.5E-02	8.1E-02	141.7	252.2
-2450	160.9	159.4	151.3	980.6	2.14	4.09E+06	6066	2.051	3.01E+17	1.11	3.4E+17	256542	0.353	2.8E-01	95.1	6.2E-02	6.5E-02	143.3	256.8
-2400	157.9	136.9	140.6	973.3	2.20	6.13E+06	13909	7.757						3.1E-03	-0.5	7.3E-04	7.3E-04	144.3	251.8
-2350	154.9	133.7	139	968.5	2.20	6.13E+06	13925	7.762						3.1E-03	-0.7	7.3E-04	7.3E-04	144.3	246.6
-2300	151.9	130.4	137.3	963.5	2.20	6.13E+06	13943	7.767						3.1E-03	-1.0	7.3E-04	7.3E-04	144.3	241.3
-2250	148.9	127.1	135.7	958.4	2.21	6.13E+06	13959	7.773						3.1E-03	-1.2	7.3E-04	7.3E-04	144.3	236.0
-2200	145.9	123.8	134	953.2	2.21	6.13E+06	13974	7.778						3.1E-03	-1.4	7.3E-04	7.3E-04	144.3	230.8
-2150	142.9	120.4	132.3	947.8	2.22	6.13E+06	13987	7.782						3.1E-03	-1.6	7.3E-04	7.3E-04	144.2	225.5
-2100	139.9	117	130.6	942.3	2.23	6.12E+06	13997	7.786						3.1E-03	-1.9	7.3E-04	7.3E-04	144.2	220.3
-2050	136.9	113.5	128.8	936.6	2.23	6.11E+06	14004	7.79						3.1E-03	-2.1	7.3E-04	7.3E-04	144.2	215.1
-2000	133.9	109.9	127	930.7	2.24	6.10E+06	14007	7.793						3.1E-03	-2.4	7.3E-04	7.3E-04	144.2	209.9
-1950	130.9	106.3	125.2	924.7	2.25	6.09E+06	14005	7.795						3.1E-03	-2.6	7.3E-04	7.3E-04	144.2	204.8
-1900	127.9	103	123.5	918.5	2.25	6.08E+06	14017	7.8						3.1E-03	-2.8	7.3E-04	7.3E-04	144.1	199.7
-1850	124.9	100.1	122.1	912.1	2.26	6.09E+06	14048	7.809						3.1E-03	-3.0	7.3E-04	7.4E-04	144.1	194.6
-1800	121.9	97.24	120.7	905.5	2.26	6.09E+06	14080	7.819						3.1E-03	-3.2	7.4E-04	7.4E-04	144.1	189.5

-1750	118.9	94.45	119.2	898.6	2.27	6.10E+06	14115	7.829						3.1E-03	-3.4	7.4E-04	7.4E-04	144.0	184.5
-1700	115.9	91.72	117.9	891.5	2.28	6.10E+06	14153	7.84						3.1E-03	-3.6	7.4E-04	7.4E-04	144.0	179.5
-1650	112.9	88.79	116.4	884.1	2.28	6.11E+06	14181	7.849						3.1E-03	-3.8	7.4E-04	7.4E-04	144.0	174.5
-1600	109.9	85.65	114.8	876.5	2.29	6.10E+06	14198	7.856						3.1E-03	-4.0	7.4E-04	7.4E-04	143.9	169.5
-1550	106.9	82.51	113.2	868.4	2.30	6.09E+06	14215	7.863						3.1E-03	-4.2	7.4E-04	7.4E-04	143.9	164.6
-1500	103.9	79.38	111.6	860.1	2.31	6.08E+06	14231	7.87						3.1E-03	-4.4	7.4E-04	7.4E-04	143.8	159.7
-1450	100.9	76.27	110	851.3	2.32	6.08E+06	14246	7.877						3.1E-03	-4.6	7.5E-04	7.5E-04	143.8	154.9
-1400	97.89	73.17	108.5	842.2	2.33	6.07E+06	14262	7.884						3.1E-03	-4.9	7.5E-04	7.5E-04	143.7	150.1
-1350	94.89	70.09	106.9	832.5	2.34	6.06E+06	14277	7.891						3.1E-03	-5.1	7.5E-04	7.5E-04	143.7	145.3
-1300	91.89	67.03	105.3	822.3	2.35	6.05E+06	14291	7.899						3.1E-03	-5.3	7.5E-04	7.5E-04	143.6	140.6
-1250	88.89	64.01	103.8	811.6	2.36	6.04E+06	14306	7.906						3.1E-03	-5.5	7.5E-04	7.5E-04	143.6	135.9
-1200	85.89	61.02	102.3	800.1	2.37	6.03E+06	14322	7.914						3.1E-03	-5.7	7.6E-04	7.6E-04	143.5	131.2
-1150	82.89	58.08	100.8	788	2.68	6.02E+06	15360	7.546						3.1E-03	-5.9	7.6E-04	7.6E-04	143.5	126.6
-1100	79.89	55.19	99.31	774.9	2.69	6.01E+06	15388	7.55						3.1E-03	-6.1	7.6E-04	7.6E-04	143.4	122.1
-1050	76.89	52.37	97.87	760.9	2.71	6.00E+06	15418	7.555						3.1E-03	-6.3	7.6E-04	7.6E-04	143.4	117.6
-1000	73.89	49.62	96.46	745.8	2.73	5.99E+06	15451	7.56						3.1E-03	-6.4	7.6E-04	7.6E-04	143.3	113.1
-950	70.89	46.95	95.1	729.3	2.74	5.98E+06	15488	7.567						3.1E-03	-6.6	7.7E-04	7.7E-04	143.2	108.8
-900	67.89	44.39	93.78	711.3	2.76	5.98E+06	15531	7.574						3.1E-03	-6.8	7.7E-04	7.7E-04	143.2	104.4

-850	64.89	41.94	92.53	691.4	2.78	5.98E+06	15580	7.583						3.1E-03	-7.0	7.7E-04	7.7E-04	143.1	100.2
-800	61.89	39.63	91.33	669.4	2.79	5.98E+06	15637	7.593						3.1E-03	-7.1	7.7E-04	7.7E-04	143.0	96.0
-750	58.89	37.46	90.22	644.7	2.81	5.98E+06	15704	7.605						3.1E-03	-7.3	7.7E-04	7.7E-04	143.0	91.9
-700	55.89	35.45	89.18	617.1	2.83	5.99E+06	15783	7.62						3.1E-03	-7.4	7.8E-04	7.8E-04	142.9	87.9
-650	52.89	33.62	88.23	586	2.85	6.01E+06	15875	7.636						3.1E-03	-7.5	7.8E-04	7.8E-04	142.8	84.0
-600	49.89	31.99	87.37	551.2	2.87	6.02E+06	15984	7.656						3.1E-03	-7.6	7.8E-04	7.8E-04	142.8	80.2
-550	46.89	30.55	86.62	513	2.88	6.05E+06	16110	7.679						3.1E-03	-7.7	7.8E-04	7.8E-04	142.7	76.5
-500	43.89	29.33	85.97	472.3	2.90	6.08E+06	16258	7.705						3.1E-03	-7.8	7.8E-04	7.8E-04	142.6	73.0
-450	40.89	28.33	85.43	430.8	2.92	6.12E+06	16430	7.736						3.1E-03	-7.9	7.8E-04	7.8E-04	142.5	69.5
-400	37.89	27.54	85	390.4	2.95	6.18E+06	16632	7.772						3.1E-03	-7.9	7.8E-04	7.8E-04	142.5	66.1
-350	34.89	26.97	84.68	352.4	2.97	6.24E+06	16867	7.815						3.1E-03	-7.9	7.8E-04	7.8E-04	142.4	62.8
-300	31.89	26.59	84.45	317.4	3.00	6.31E+06	17144	7.865						3.1E-03	-8.0	7.8E-04	7.8E-04	142.3	59.6
-250	28.89	26.38	84.31	285.3	3.03	6.39E+06	17470	7.924						3.1E-03	-8.0	7.8E-04	7.8E-04	142.2	56.3
-200	25.89	26.3	84.24	255.9	3.07	6.49E+06	17854	7.994						3.1E-03	-8.0	7.8E-04	7.8E-04	142.2	53.0
-150	22.89	26.31	84.21	228.6	3.11	6.61E+06	18307	8.078						3.1E-03	-8.0	7.7E-04	7.7E-04	142.1	49.6
-100	19.89	26.41	84.22	203.1	3.17	6.74E+06	18856	8.182						3.1E-03	-8.0	7.7E-04	7.7E-04	142.0	46.1
-50	16.89	26.61	84.29	178.9	3.24	6.91E+06	19552	8.316						3.1E-03	-7.9	7.7E-04	7.7E-04	142.0	42.5
0	13.89																	141.9	38.6

APPENDIX C

AN EXAMPLE FOR RANKINE CYCLE CALCULATION BY USING EES SOFTWARE

Stages	T (ºC)	P kPa	h (kJ/kg)	s (kJ/kgK)	$\dot{m}$ kg/s	$W_{turbine}$	W_{gen}	W_{pump}	W_{net}
						(kW)			
1	141.9	3860	351.6	1.054	64				
2	67.98	668.8	306.8	1.054	64	2867	2723	211.7	2511
3	25.15	668.8	86.62	0.325	64				
4	27.12	708.8	89.43	0.3343	64				